Journal of
Materials Chemistry B

REVIEW

View Article Online
View Journal | View Issue

Check for updates

Cite this: J. Mater. Chem. B, 2019, 7, 5583

Layered double hydroxide nanostructures and nanocomposites for biomedical applications

Li Yan,[c] Sevil Gonca,[b] Guangyu Zhu,[e] Wenjun Zhang[d] and Xianfeng Chen*[ab]

Received 28th June 2019,
Accepted 24th August 2019

DOI: 10.1039/c9tb01312a

rsc.li/materials-b

Layered double hydroxide (LDH) nanostructures and related nanocomposites have attracted significant interest in biomedical applications including cancer therapy, bioimaging and antibacterial treatment. These materials hold great advantages including low cost and facile preparation, convenient drug loading, high drug incorporation capacity, good biocompatibility, efficient intracellular uptake and endosome/lysosome escape, and natural biodegradability in an acidic environment. In this review, we summarize the development of three types of LDH nanostructures including pristine LDH, surface modified LDH, and LDH nanocomposites for a range of biomedical applications. The advantages and disadvantages of LDH nanostructures and insights into the future development are also discussed.

Open Access Article. Published on 29 August 2019. Downloaded on 2/10/2026 5:01:13 AM.
This article is licensed under a Creative Commons Attribution 3.0 Unported Licence.

1. Introduction

Layered double hydroxides (LDH) are a type of anionic clay with the formula generally expressed as $[M_{1-x}^{2+}M_x^{3+}(OH)_2][A^{n-}]_{x/n}\cdot zH_2O$, where divalent cations M^{2+} are Mg^{2+}, Fe^{2+}, or Co^{2+}; trivalent cations M^{3+} are Al^{3+}, Fe^{3+}, or Gd^{3+}; and non-framework and exchangeable anions A^{n-} are Cl^-, CO_3^{2-}, NO_3^-, *etc.*[1–5] (Fig. 1). LDH are positively charged because M^{2+} anions are partially substituted by M^{3+}. LDH nanostructures have been widely utilized for many applications, including energy, healthcare, catalysis and optics. This review will focus on the biomedical applications of LDH nanostructures and nanocomposites. Herein, we classify LDH nanostructures into 3 categories including pristine LDH nanostructures, surface modified LDH nanostructures including nanoparticles and recently reported nanosheets, and LDH nanocomposites. These LDH nanomaterials are useful for a range of biomedical applications (Fig. 2). For example: (1) –OH groups make LDH sensitive to an acid environment and degrade easily in the biological environment to release loaded therapeutic molecules for bio-responsive drug delivery and (2) the positive charge of LDH allows the material to effectively interact with negatively charged cell membranes for efficient intracellular delivery. Due to the broad applications, LDH nanostructures are increasingly attractive and the synthesis, characterization and applications of LDH have undergone rapid development during the last decade.[6–11] The number of

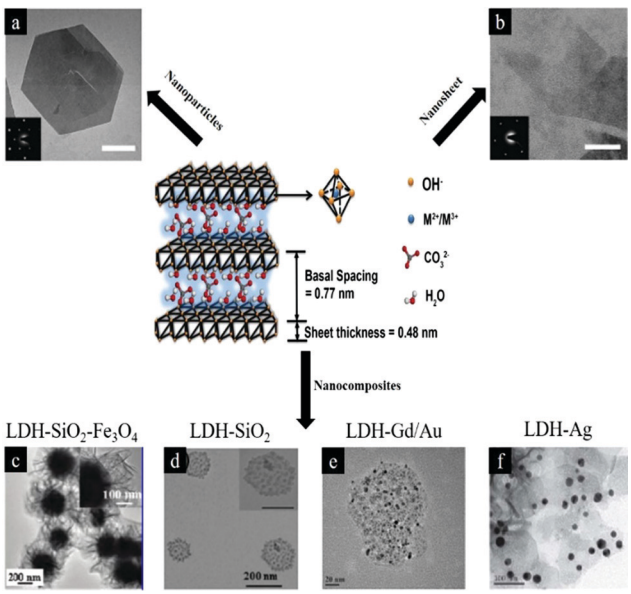

Fig. 1 Schematic illustration of LDH structure and chemical components[6] (reproduced from The Royal Society of Chemistry with permission). (a) LDH nanoparticles[7] (reproduced from Macmillan Publishers Limited with permission), (b) LDH nanosheets[7] (reproduced from Macmillan Publishers Limited with permission), (c–f) LDH nanocomposites (reproduced from American Chemical Society, Springer, Elsevier and The Royal Society of Chemistry with permission).[8–11]

[a] Translational Medicine Center, The Second Affiliated Hospital, Guangzhou Medical University, Guangzhou, P. R. China
[b] School of Engineering, Institute for Bioengineering, The University of Edinburgh, King's Buildings, Mayfield Road, Edinburgh EH9 3JL, UK. E-mail: Michael.Chen@ed.ac.uk
[c] Monash Institute of Pharmaceutical Sciences, Monash University, Parkville, Victoria 3052, Australia
[d] Center of Super-Diamond and Advanced Films (COSDAF) and Department of Materials Science and Engineering, City University of Hong Kong, Hong Kong SAR, P. R. China
[e] Department of Chemistry, City University of Hong Kong, Hong Kong SAR, P. R. China

Open Access Article. Published on 29 August 2019. Downloaded on 2/10/2026 5:01:13 AM.
This article is licensed under a Creative Commons Attribution 3.0 Unported Licence.

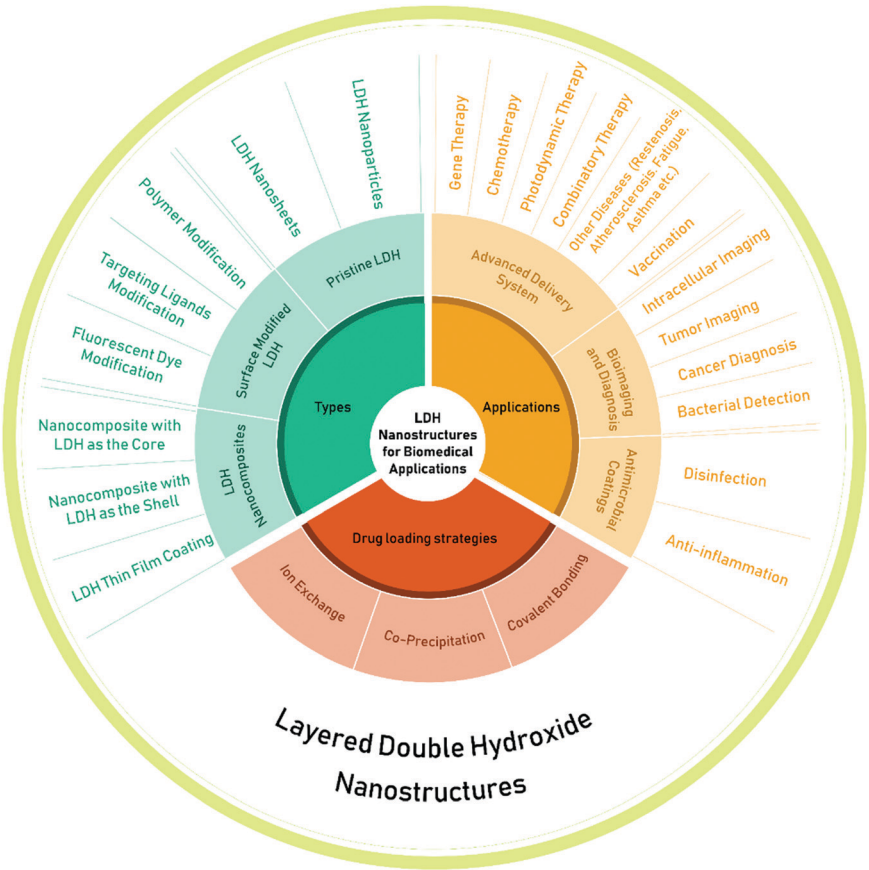

Fig. 2 The types, drug loading strategies and applications of layered double hydroxide (LDH) nanostructures.

publications on LDH in both general and specific biomedical applications is increasing every year.

Pristine LDH nanoparticles were initially introduced for drug and gene delivery for cancer chemotherapy and then LDH nanostructures with different morphologies and geometries were developed for a wider range of applications. During this journey, to satisfy the requirements of advanced drug delivery systems and different biomedical applications, surface modified LDH nanostructures and LDH based nanocomposites have also been explored. In this review, we summarize and highlight the most important development of these three types of LDH nanostructures for biomedical applications, discuss about their advantages and disadvantages, and also provide our insights into the challenges and future applications of LDH nanomaterials.

2. Pristine LDH nanostructures for drug and gene delivery

Biological barriers in the human beings can effectively restrict hazardous agents and thus protect them from harmful diseases. As one of the most common biological barriers, the cell membrane can isolate, protect and regulate cells from the external environment.[12–16] However, the fine and sophisticated structure of the cell membrane unavoidably and strictly prohibits the transport of drugs and genes into the cytoplasm and nucleus, resulting in minimal or even negligible delivery efficiency.[17] To address this problem, methods including biological,[18–22] chemical,[23–27] and physical approaches[28–33] have been extensively developed. Among these technologies, nanomaterials show great potential to permeate the cell membrane and greatly increase drug delivery efficiency with low toxicity.[34–41] Besides drug delivery application, nanostructures are also broadly used for other biomedical applications such as bioimaging, sensing, and separating protein/harmful agents.[42–46]

2.1 Cancer therapy and drug delivery

Pristine LDH nanoparticles were first introduced in the 2000s as a nonviral vector for biomolecule and deoxyribonucleic acid (DNA) delivery by Choy and co-workers.[47] In 2004, Choy *et al.* reported that pristine LDH nanoparticles could load negatively charged drug molecules for cancer therapy.[48] Methotrexate (MTX) was loaded into the interlayer space of LDH nanoparticles by mixing LDH with MTX at room temperature for 3 days through ion-exchange by replacing the NO_3 ions. After drug loading, the interlayer space of LDH nanoparticles expanded from 8.4 to 19.9 Å, but the structure and function of MTX and LDH nanoparticles were maintained without detectable change. The *in vitro* cell line test results showed that MTX-LDH nanoparticles were effective sooner than MTX alone. With 24 hours co-incubation of cell lines and drugs, the viability of

 This journal is © The Royal Society of Chemistry 2019

Open Access Article. Published on 29 August 2019. Downloaded on 2/10/2026 5:01:13 AM. This article is licensed under a Creative Commons Attribution 3.0 Unported Licence.

the cancer cells treated with MTX remained over 90%; in comparison, the viability of cells in the MTX-LDH treated group dropped to below 80%. Attractively, MTX-LDH nanoparticles effectively suppressed the proliferation of SaOS-2 cancer cells (osteosarcoma, human), but showed a negligible effect on normal cells (fibroblasts, human tendon). This work first demonstrated that LDH nanoparticles could act as a biocompatible non-viral vector for enhanced anti-cancer drug delivery.

The effectiveness of using LDH nanoparticles for drug delivery and the attractive cancer cell killing specificity were later demonstrated also in cisplatin prodrug delivery.[49] In terms of drug delivery effectiveness, disuccinatocisplatin (DSCP)-loaded LDH nanoparticles exhibited dramatically higher cytotoxicity than the free prodrug: the IC_{50} value of DSCP against A2780 cancer cells was 1.75 ± 0.20 μM, while the value was 0.34 ± 0.17 μM for LDH–Pt(IV) (LDH nanoparticles loaded with DSCP), indicating a 5-fold reduction of the IC_{50} value (Table 1). With regard to cell specificity, LDH-Pt(IV) nanoparticles were significantly less effective towards the tested normal cells (NIH3T3, HS27 and BEAS-2B). For example, the IC_{50} values of cisplatin and DSCP were 5.1 ± 0.8 and 30 ± 2 μM, respectively, while the value of LDH–Pt(IV) was over 50 μM. These comparisons indicate that DSCP-loaded LDH nanoparticles are very effective in killing cancer cells, but relatively safe to healthy cells, which is ideal for anticancer drug design. To explain the cancer cell targeting specificity, the platinum content of cells was investigated after incubation with DSCP and DSCP-LDH. It was found that LDH-Pt(IV) could deliver 10-fold more drug to cells compared to DSCP alone.

Following the test in cell lines, Choi *et al.* studied MTX-LDH nanoparticles with an average diameter of 130 nm for *in vivo* cancer therapy.[50] Free MTX and MTX-LDH nanoparticles were intraperitoneally injected into two groups of mice bearing orthotopic human breast tumors. In the biodistribution analysis, it was discovered that the tumor–liver drug accumulation ratio of the MTX-LDH nanoparticle treated group was 6 times higher than that of the MTX-treated group. In line with this LDH nanoparticle enabled targeted delivery of MTX to the tumor, the antitumor efficacy of the nanoparticle treated group was significantly improved, indicated by 81.4% and 74.3% reductions of tumor volumes compared with that in the phosphate buffered saline (PBS) and free MTX group, respectively. This also shows that the efficacy of free drug is very low.

Besides cancer chemotherapy, LDH nanoparticles were also utilized as a photosensitizer vector for photodynamic therapy. Duan and co-workers reported that the incorporation of zinc phthalocyanine (ZnPc) into the gallery of LDH nanoparticles resulted in high singlet oxygen production efficiency, improved photostability, good biocompatibility and low cytotoxicity.[51] The *in vitro* test showed that a low dosage of ZnPc (10 μg mL^{-1}) caused potent damage to HepG2 cells with less than 15% viability. The *in vivo* investigation demonstrated that LDH nanoparticles effectively inhibited tumor growth with an ultra-low dose of 0.3 mg kg^{-1} and a low optical fluence rate of 54 J cm^{-2}. Recently, Mei *et al.* reported two-dimensional LDH monolayers with a diameter of 50 nm and a thickness of 0.8 nm for controlled loading and targeted delivery for cancer therapy.[52] In this research, monolayered LDH nanosheets were loaded with the anticancer drug doxorubicin (DOX) with a high loading capacity of 3.6 mg mg^{-1} (DOX/LDH). The fabricated nanovectors, which could be further conjugated with the targeting agent folic acid, exhibited selective high toxicity towards cancer cells (KB cancer cells) and reduced toxicity to normal cells.[52] Gao *et al.* developed a supramolecular photosensitizer (isophthalic acid/LDH nanohybrids) that could be activated by a near-infrared laser for efficient two-photon photodynamic therapy.[53] Upon 808 nm laser irradiation, this LDH based hybrid demonstrated significantly increased tissue penetration depth and was capable of killing cancer cells inside the tumor.[53]

Beyond cancer therapy, LDH nanoparticles have also been applied to many other applications.[54] For example, to overcome the limitation of the short half-life of the anticoagulant drug low molecular weight heparin (LMWH), LMWH-LDH nanoparticles were fabricated *via* a co-precipitation method (adding drug simultaneously during the LDH nanoparticle preparation process, instead of preparing LDH nanoparticles first followed by drug loading *via* ion-exchange).[55] The *in vitro* release test indicated a biphasic and sustainable release profile of LMWH-LDH nanoparticles in pH 7.4 PBS solution at 37 °C. The liberation of the anticoagulant drug was 20% in the first 12 hours, followed by a further 20% release in the following 108 hours. The same group also found that LMWH-LDH nanoparticles had the potential to treat restenosis of an artery that occurs after surgically removing atherosclerotic lesions and restoring blood flow.[56] Restenosis is the recurrence of blood vessel narrowing. LMWH-LDH nanoparticles were tested on rat vascular smooth muscle cells (SMC): LMWH-LDH nanoparticles showed a higher ability to inhibit the migration and proliferation of SMC, with over 60% reduction of SMC compared with the control group (only growth medium). The enhanced efficacy of LMWH-LDH nanoparticles was explained as

Table 1 IC_{50} values of cisplatin, DSCP, LDH-Pt(IV), and LDH in different cell lines[49] (reproduced from The Royal Society of Chemistry with permission)

Cell type	Cell line	Cisplatin [μM]	DSCP [μM]	LDH-Pt(IV) [μM]	LDH [mg L^{-1}]
Cancer	A549	5.0 ± 0.4	9.8 ± 0.2	0.84 ± 0.28	>150
Cancer	A2780	0.45 ± 0.1	1.8 ± 0.2	0.34 ± 0.17	>150
Cancer	NCI-H1299	3.3 ± 0.4	4.2 ± 0.7	0.71 ± 0.07	N.D.
Cancer	MCF-7	17 ± 1	>25	1.9 ± 0.6	N.D.
Cancer	HCT116	3.7 ± 0.5	12 ± 1	0.49 ± 0.03	N.D.
Normal	NIH3T3	5.1 ± 0.8	30 ± 2	>50	>150
Normal	HS27	7.6 ± 0.7	35 ± 2	>50	N.D.
Normal	BEAS-2B	2.7 ± 0.2	4.6 ± 0.9	23 ± 1	45

Open Access Article. Published on 29 August 2019. Downloaded on 2/10/2026 5:01:13 AM.
This article is licensed under a Creative Commons Attribution 3.0 Unported Licence.

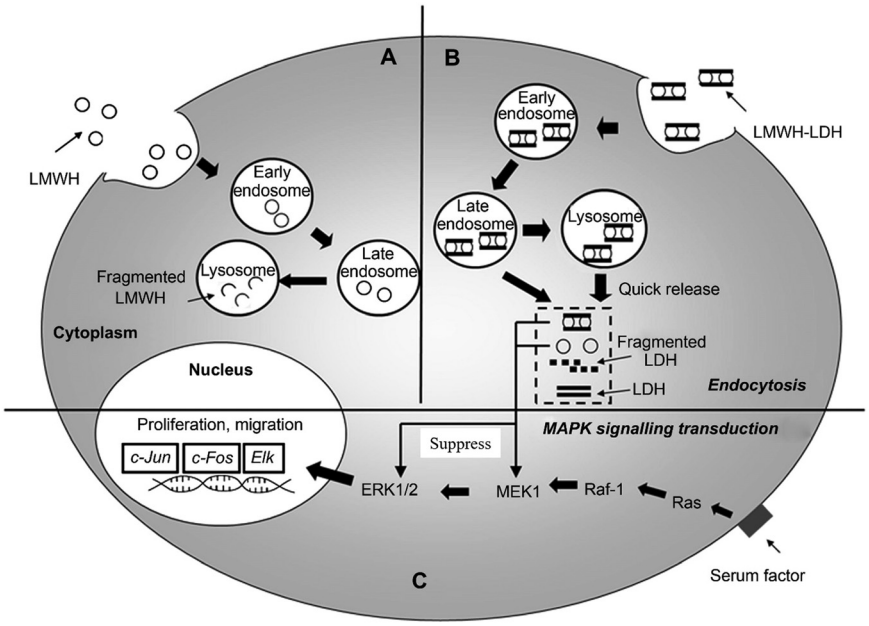

Fig. 3 Schematic diagram showing the proposed intracellular trafficking of LMWH-LDH nanoparticles in SMC. Both LMWH (A) and LMWH-LDH (B) are internalized by SMC *via* endocytosis; however, LMWH-LDH has the capacity of 'endosomal escape' preventing the degradation of LMWH in lysosomal compartments. LMWH-LDH and LMWH act to inhibit the MAPK pathway.[57] (Reproduced from Elsevier with permission.)

due to the higher cellular uptake through the endocytic pathway, quick escape from late endosomes/lysosomes, and effectively inhibited mitogen-activated protein kinase (MAPK) signal transduction over a prolonged period of time[57] (Fig. 3). LMWH delivery by LDH vectors was further improved by using antibody-targeted LDH nanoparticles for atherosclerosis.[58] In the system, an antibody (H93.7C.1D2/48; 1D2) was covalently conjugated to LMWH to form the 1D2–LMWH complex. Subsequently, this 1D2–LMWH complex was loaded into LDH nanoparticles *via* electrostatic interaction. The results showed that this nanodrug delivery system could be effectively transported to the arterial injury site with the aid of a targeting antibody, consequently achieving the sustained release of LMWH and resulting in minimized luminal loss and reduced thrombotic occlusion in a rat model of arterial injury.

Additionally, LDH nanoparticles were employed as an adjuvant to promote Th1 or Th2 dominant immune responses for vaccination purpose.[59] LDH nanoparticles were conjugated with a toll-like receptor ligand CpG, leading to significantly enhanced antibody response and a switch from Th2 towards Th1 response. On Day 21, LDH delivery induced significantly higher IgG2a antibody response than a standard commercial adjuvant Alum. Moreover, the animal test showed that immunization of mice with CpG-OVA-conjugated LDH nanoparticles before challenging with OVA-expressing B16/F10 tumor cells retarded tumor growth and prolonged the survival of tumor-bearing mice.[59] Furthermore, LDH nanoparticles loaded with the antigen Intimin β showed significantly enhanced uptake by antigen-presenting cells, promoting immune responses against infections by diarrheagenic *E. coli*.[60] LDH nanoparticles with Intimin β induced strong antibody- and cell-mediated immune responses, which maintained for at least four months in the mouse model with no changes in the histopathology of the animal organs.

Very recently, LDH nanoparticles were used for *in vivo* anti-fatigue by incorporating folic acid.[61] LDH-folic acid constructs were fabricated *via* a co-precipitation method. It was found that the constructs were able to prolong the forced swimming time of the tested mice by 32% and 51% in comparison with the folic acid group and the control, with negligible cytotoxicity to normal cells. The forced swimming test was used to evaluate the mice's physical endurance capacity: reduced susceptibility to fatigue was correlated with longer swimming times.[56] Interestingly, it was also found that LDH-folic acid had an obvious effect on decreasing blood urea nitrogen and blood lactic acid, and increasing muscle and hepatic glycogen levels. These results indicated that LDH-folic acid effectively protected the body from fatigue. Wang *et al.* reported dexamethasone sodium phosphate (Dexa)-LDH nanoparticles for asthma treatment.[62] In the allergic asthma rat model, this nanostructure effectively reduced inflammatory cells (macrophages, eosinophils and neutrophils) in the bronchoalveolar lavage (BAL) fluid, inhibited the increase of T-helper-2-type cytokines, and suppressed airway hyperresponsiveness.

For biomedical applications, it is essential for materials to have minimal toxicity. To know this, the bio-safety of LDH nanoparticles was investigated *in vivo*.[63] The study demonstrated that, when LDH nanoparticles were intravenously injected to Sprague Dawley rats at a dose of below 200 mg kg^{-1}, no obvious systemic side-effect could be observed in clinical chemistry and histopathology. This study confirmed the excellent biocompatibility of LDH nanoparticles and indicated their promising applications in biomedicine. The effectiveness and biocompatibility of LDH nanostructures can be controlled through various designs. When tested in mammalian cell lines,[59] it was found LDH nanostructures were rapidly uptaken by cells, and the shape had an influence on their

 This journal is © The Royal Society of Chemistry 2019

Open Access Article. Published on 29 August 2019. Downloaded on 2/10/2026 5:01:13 AM.
This article is licensed under a Creative Commons Attribution 3.0 Unported Licence.

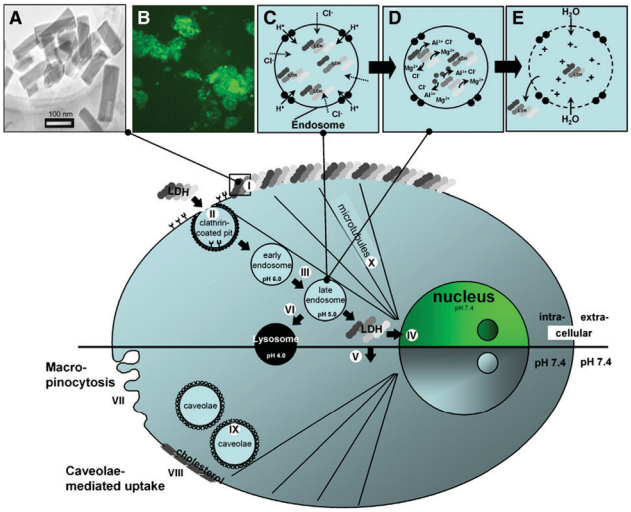

Fig. 4 Schematic illustration of LDH-FITC nanoparticle endocytosis and cellular trafficking. (A) TEM image of LDH-FITC nanoparticles; (B) CHO cells after addition of LDH-FITC nanoparticles to the cell culture medium; (C) pumping protons into the endosome to facilitate acidification for subsequent proteolysis of nutrients, followed by an influx of chloride ions; (D) acid-driven dissolution of LDH-FITC nanoparticles in the late endosome to buffer acidification and release many ions; (E) entrance of water molecules to the endosome due to an increase in ionic strength, leading to osmotic swelling and endosome burst which releases LDH-FITC nanoparticles into the cytoplasm. Step (I): Adhesion of LDH-FITC nanoparticles to the cell membrane; (II) clathrin-mediated endocytosis; (III) endosomal changes; (IV) nuclear localization of LDH-FITC; (V) cytoplasmic distribution of LDH-FITC; (VI) lysosomal pathway; (VII) unspecific uptake through macropinocytosis; (VIII and IX) caveolae-mediated endocytosis; (X) microtubule directing the freed LDH-FITC nanoparticles to the nucleus.[64] (Reproduced from Elsevier with permission.)

distribution in cells: rod-like LDH could target the nucleus, while sheet-like LDH were retained in the cytoplasm. The intracellular uptake process of LDH nanostructures was assumed to be happening through a number of steps including quick adhesion of the material to the cell membrane, clathrin-mediated endocytosis to enter cells, and endosomal/lysosomal escape to the cytoplasm. For rod-like LDH nanoparticles, there is an extra step of nuclear translocation[64] (Fig. 4). Recently, Senapati *et al.* loaded a hydrophobic anticancer drug, raloxifene hydrochloride (RH), into a series of Mg–Al LDH nanoparticles with various charge density anions through the ion exchange technique for controlled drug delivery.[65] Through this, the release profiles of RH could be tuned from fast to sustained release by altering the exchangeable anions: nitrate incorporated LDH nanoparticles allowed interaction with the loaded drug and consequently led to sustained drug delivery; in comparison, the phosphate incorporated LDH–drug system exhibited fast release of drug due to loose interactions between LDH nanoparticles and drug molecules. The *in vivo* study suggested that the LDH–drug system with slow release profiles was a safer nanovector for cancer therapy.

2.2 Gene delivery

Gene therapy has attracted scientists and clinicians for treating diseases using therapeutic nuclei acids, such as DNA, small interfering RNA (siRNA) and microRNA (miRNA).[66–73] For example, siRNA showed great potential for cellular therapy of neurodegenerative disorders,[74–76] cancers[77–79] or infectious diseases.[80,81] However, the success of gene therapy was hindered by limitations such as ease of degradation, low efficiency of delivery, and high toxicity in systemic transport. To solve these problems, LDH nanoparticles have been used for gene delivery since 2000s. This material could protect the gene from degradation and also enhance intracellular delivery efficacy.[82] Li *et al.* discovered that 20 nm LDH nanoparticles could effectively enter both the cytoplasm and cellular nucleus, while large (180 nm) ones only located in the cytoplasm.[83] Therefore, 20 nm LDH nanoparticles were used to deliver the pEGFP-N1 DNA plasmid to transfect NSC 34 cells with minimal cell death. Although LDH nanoparticles could be used for gene delivery, the transfection efficiency was found to be generally low because of the large size of DNA.[84] For this reason, LDH nanoparticles would be more suitable for siRNA delivery.[85,86] In one study, LDH-siRNA displayed greatly enhanced intracellular delivery of siRNA to mammalian cells[86] and cortical neurons.[85] The intracellular uptake of LDH-siRNA was demonstrated to be through clathrin-mediated endocytosis. As shown in Fig. 5a, in the absence of chlorpromazine (a clathrin-mediated endocytosis inhibitor), strong fluorescence signals (siRNA duplex was covalently coupled to 6FAM fluorophore at the 5′ end) were observed in cells at 40 min after incubation (Fig. 5a–i). In great contrast, in the presence of chlorpromazine, significantly diminished fluorescence signals were found within the neuronal cytoplasm. These observations indicated that clathrin-mediated endocytosis played an important role in LDH internalization.[86]

LDH nanoparticles also show promise for topical application of RNA interference for sustained protection against plant viruses.[87] Pathogen-specific double-stranded RNA (dsRNA) can protect plants from viral infection, but its instability limits the application. To address this problem, dsRNA was loaded on LDH nanoparticles. The results demonstrated that the stability of dsRNA could be improved and the dsRNA was able to be slowly released even 30 days after spraying on plant leaves. Very attractively, a single spray of dsRNA loaded on LDH nanoparticles on plant leaves enabled virus protection for at least 20 days (Fig. 5b and c).

2.3 Co-delivery of drugs/genes and bioimaging

Simple delivery of one kind of drug is sometimes not able to satisfy the requirement of an advanced drug delivery system. Taking cancer therapy as an example, multiple drugs are often used to have different targets such as targeting both nucleus DNA and mitochondrial membranes, allowing much improved therapeutic efficacy and alleviated drug resistance.[88,89] Therefore, combination therapy (delivery of two or more types of drugs) has received increasing attention.[90–92]

For this, LDH nanoparticles have been developed to simultaneously transport two types of cancer treatment agents to improve cancer therapy and overcome drug resistance.[93] In one example, LDH nanoparticles were used as a vector to deliver the anticancer drug 5-Fluorouracil (5-Fu) and Allstars Cell Death siRNA (CD-siRNA) for potent cancer treatment.[94] The experiment outcomes proved

Open Access Article. Published on 29 August 2019. Downloaded on 2/10/2026 5:01:13 AM.
This article is licensed under a Creative Commons Attribution 3.0 Unported Licence.

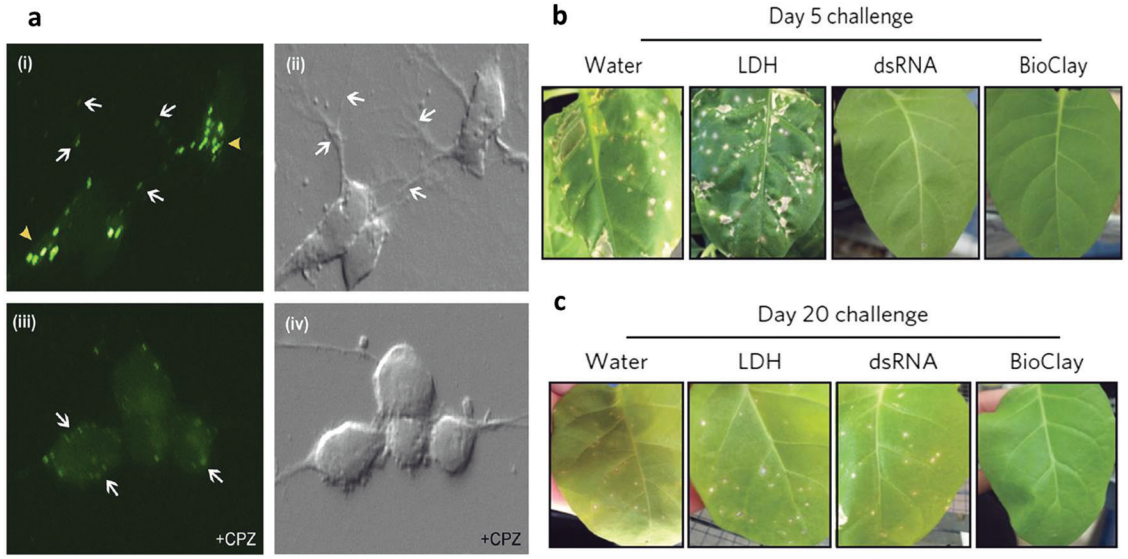

Fig. 5 (a) siRNA-LDH nanoparticles are internalized by clathrin-mediated endocytosis. Confocal images show a large number of brightly fluorescent puncta throughout the cytoplasm of neurons (arrowheads) and along their extended neurites (arrows) when incubated with siRNAeHtte6FAMeLDH complexes (i). In the presence of chlorpromazine (CPZ) (an inhibitor of clathrin-mediated endocytosis) few 6FAM-positive vesicles are seen in the neurons (iii). However, faint 6FAM-positive puncta are visible at the plasma membrane (arrows). Panels (ii) and (iv) are the corresponding bright field images of panels (i) and (iii), respectively.[86] (Reproduced from Elsevier with permission.) (b and c) Images showing the extent of necrotic lesions on N. *tabacum* cv. Xanthi leaves challenged with PMMoV 5 days post spray treatment (b) and 20 days post spray treatment (c). $*p < 0.05$, $**p < 0.01$ and $***p < 0.001$ are significant using the Kruskal–Wallis test with a post-hoc Nemenyi test for multiple comparisons between samples compared with LDH. Data represent mean ± s.e.m.[87] (Reproduced from Macmillan Publishers Limited with permission.)

that the combined chemotherapy and gene therapy significantly enhanced the cytotoxicity of 5-Fu in three cancer cell lines (MCF-7, U2OS and HCT-116). In addition, LDH nanoparticles were reported to simultaneously load a Pt(IV) prodrug and a p53 activator.[95] It was discovered that the *in vitro* anticancer activity of cisplatin in p53-wild type cells was dramatically enhanced. The introduction of active p53 protein promoted apoptotic pathways initiated by platinum drugs, thereby substantially increasing the efficacy of the cisplatin prodrug (Fig. 6). Wang *et al.* co-loaded Pt(IV) prodrugs and the Chlorin e6 (Ce6) photosensitizer into LDH nanoparticles to overcome the drug resistance of cisplatin.[96] Ce6 photosensitizer and Pt(IV) prodrugs loaded LDH nanoparticles exhibited a synergistic effect in killing cancer cells, and particularly, were highly active towards cisplatin-resistant cells, showing up to 190-fold increased efficiency in comparison with cisplatin alone. It is well known that the failure of cancer chemotherapy could be attributed to the escape of cancer cells from the immune system. In order to tackle this problem, Wang *et al.* fabricated a cisplatin-loaded immunochemotherapeutic LDH nanohybrid that bears an immune checkpoint inhibitor for enhanced cancer therapy[97] (Fig. 7). In the study, LDH nanoparticles were co-loaded with the first line chemotherapy drug cisplatin and the immune checkpoint inhibitor indoleamine-2,3-dioxygenase (IDO) inhibitor. The *in vitro* cervical cancer cell study revealed improved cellular accumulation, increased binding of Pt to DNA and higher apoptosis. The IDO inhibitor could inhibit indoleamine-2,3-dioxygenase and activate T cells, thus ultimately boosting the anti-tumor performance of the nanohybrid.[97]

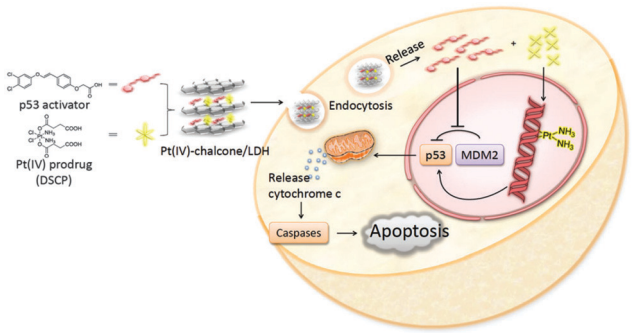

Fig. 6 Schematic illustration of co-delivery of a Pt(IV) prodrug and a p53 activator to enhance the anticancer activity of cisplatin[95] (reproduced from The Royal Society of Chemistry with permission).

Most recently, LDH has been fabricated as a multifunctional drug carrier for theranostic applications.[98–101] For instance, Li *et al.* reported pH-ultrasensitive Mn(II)-containing LDH nanoparticles with superb longitudinal relaxivity (9.48 mM^{-1} s^{-1} at pH 5.0 and 6.82 mm^{-1} s^{-1} at pH 7.0 *vs.* 1.16 mm^{-1} s^{-1} at pH 7.4) for magnetic resonance imaging (MRI).[102] A two-step method was utilized to synthesize Mn-LDH: Mg_3Al-LDH nanoparticles were first obtained through a co-precipitation method followed by isomorphic substitution of partial number of Mg^{2+} with Mn^{2+} ions (Fig. 8). The *in vivo* study revealed that Mn-LDH nanoparticles exhibited clear MRI for tumor tissues in mice for up to 2 days post intravenous injection, and also these nanoparticles were very promising for cancer diagnosis and treatment. Furthermore, Peng *et al.* prepared Gd^{3+}-doped monolayered LDH nanosheets with controlled composition and morphology,[100]

 This journal is © The Royal Society of Chemistry 2019

Open Access Article. Published on 29 August 2019. Downloaded on 2/10/2026 5:01:13 AM.
This article is licensed under a Creative Commons Attribution 3.0 Unported Licence.

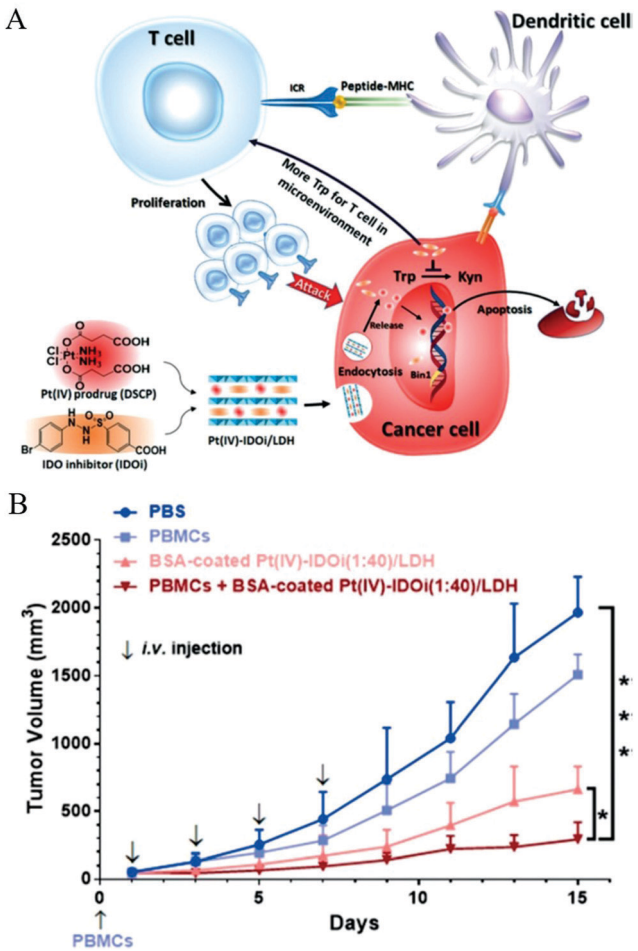

Fig. 7 (A) Strategic overview of a cisplatin-loaded nanohybrid for immunochemotherapy. The nanohybrid Pt^{IV}-IDOi/LDH enters cancer cells and releases the Pt^{IV} prodrug and IDOi. The former is reduced to cisplatin that binds to genomic DNA to induce cancer cell apoptosis; simultaneously, the latter blocks the pathway to produce kynurenine, leaving more tryptophan in the microenvironment for T cell proliferation and development. With the checkpoint inhibitor IDOi, proliferated T cells can distinguish cancer cells through the signal from antigen presenting cells (APC, such as dendritic cells), and enhance the chemotherapy. At last, the nanohybrid elevates cancer cell cycle arrest and apoptosis. IDO = indoleamine-2,3-dioxygenase, TCR = T cell receptor, MHC = major histocompatibility complex, Trp = tryptophan, Kyn = kynurenine. (B) The growth of HeLa tumors in a xenograft model with various treatment groups indicated. PBMCs (5×10^6 cells per mouse) were injected intravenously on Day 0. BSA-coated Pt^{IV}–IDOi (1 : 40)/LDH ([Pt] = 0.5 mg kg^{-1}) was injected for 4 times. The tumor volume of each group was measured every two days for 14 days of duration. $*p < 0.05$, $***p < 0.001$, Student's t-test. Mean ± SD, $n = 5$.[97] (Reproduced from Wiley-VCH Verlag GmbH & Co. KGaA with permission.)

and loaded the nanosheets with DOX (chemotherapy drug) and indocyanine green (photodynamic and photothermal agent) with a high loading content of 797.36% and an encapsulation efficiency of 99.67%. The *in vitro* and *in vivo* study demonstrated trimode (chemotherapy, photodynamic and photothermal therapy) synergetic anticancer activity with good biocompatibility. Meanwhile, Gd^{3+}-doped monolayered LDH nanosheets could be utilized as dual mode imaging (near-infrared fluorescence and magnetic resonance imaging) agents to visualize the tumor site with minimal invasion.[100] This example well demonstrates the powerful function for drug delivery and integrated treatment and diagnosis.

3. Surface modified LDH for biomedical applications

Although LDH nanoparticles are widely used as a vector for enhanced drug and gene delivery, the vast majority of studies have been based on as-prepared pristine (non-surface modified) LDH structures. However, these pristine nanoparticles often suffer from problems of instability in *in vivo* applications due to the lack of surface stabilization. Moreover, besides increasing the stability of LDH nanoparticles, surface modification plays an extremely important role in using nanomaterials for biomedical applications.[103–107] Firstly, surface modification allows convenient attachment of targeting ligands to nanostructures for targeted delivery. Secondly, surface modification renders nanomaterials flexibility in drug loading and versatile functionalities. Thirdly, surface modification is very important for enhancing nanomaterials' cellular uptake, stability, and biocompatibility.

For this purpose, surface modified and exfoliated layered gadolinium hydroxide nanoparticles were developed for use as multimodal contrast agents for MRI and fluorescence imaging.[108] In this material, LDH nanoparticles contain MR-active Gd^{3+} ions, which makes the material have potential for MRI. Then LDH nanoparticles were exfoliated by incorporation of long chain oleate ions, as shown in Fig. 9a. The separate individual layers were coated with phospholipids with poly(ethylene glycol) tail groups and fluorescent molecules to achieve multimodal imaging (MRI + fluorescence imaging) application *in vivo* (Fig. 9a). In another work, LDH nanoparticles were coated with liposome, enabling excellent water dispersion and sustained release characteristic, as shown in Fig. 9b.[109] Recently, the bovine serum albumin (BSA) precoating strategy was introduced to increase LDH nanoparticles' stability in buffered solution. This coating strategy could substantially prevent aggregation of LDH nanoparticles, and increase their cellular uptake in Chinese hamster ovary cells.[110] Shi *et al.* fabricated bivalent cation $^{64}Cu^{2+}$ and trivalent cation $^{44}Sc^{3+}$ labelled LDH nanoparticles-BSA nanoparticles with excellent labelling efficiency and stability for *in vivo* positron emission tomography (PET).[111] In this work, PET imaging showed that prominent tumor uptake was achieved in 4T1 breast cancer with ^{64}Cu-LDH nanoparticles-BSA *via* passive targeting alone (7.7 ± 0.1% ID g^{-1} at 16 h post-injection; $n = 3$). Zuo *et al.* modified LDH nanoparticles with brain tumor targeting ligands angiopep-2 and rabies virus glycoprotein.[112] The ligands were first covalently linked with BSA through the heterobifunctional cross-linker sulfosuccinimidyl 4-(*N*-maleimidomethyl)cyclohexane-1-carboxylate, and then coated onto the surface of LDH nanoparticles through electrostatic interaction, followed by cross-linking with the cross-linker glutaraldehyde to immobilize these BSAs on the LDH nanoparticles' surface. The ligand conjugated LDH nanoparticles showed dramatically enhanced cellular uptake by

Open Access Article. Published on 29 August 2019. Downloaded on 2/10/2026 5:01:13 AM.
This article is licensed under a Creative Commons Attribution 3.0 Unported Licence.

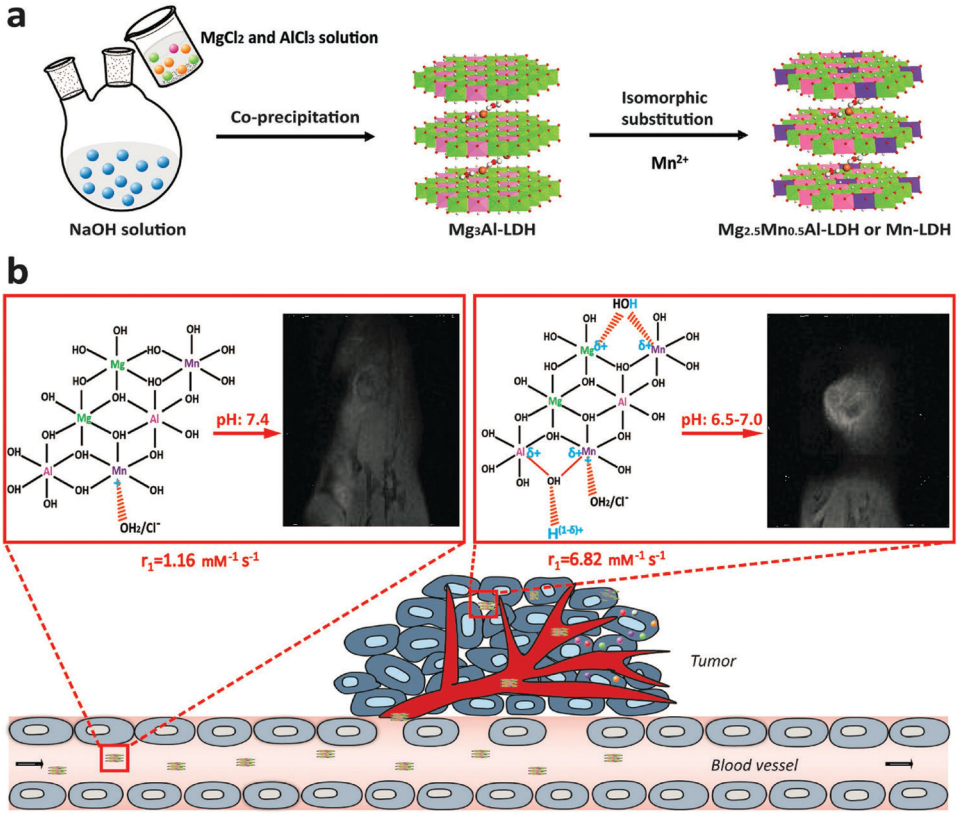

Fig. 8 Schematic illustration of (a) the synthetic procedure and (b) structure related multifunctional properties of Mn-LDH nanoparticles.[102] (Reproduced from Wiley-VCH Verlag GmbH & Co. KGaA with permission.)

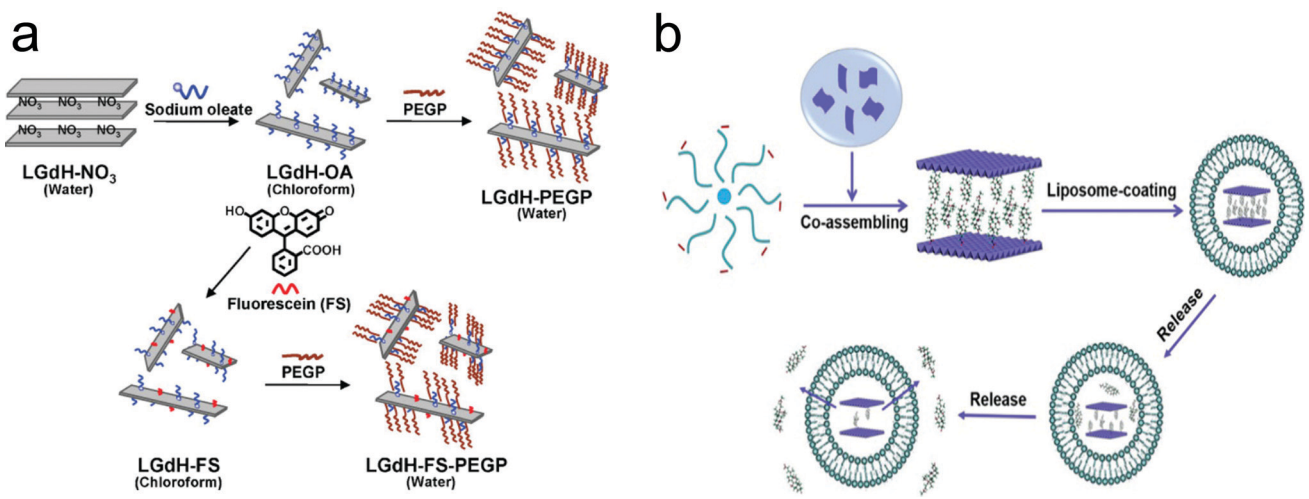

Fig. 9 The surface modification approach for the fabrication of (a) exfoliated layered gadolinium hydroxide[108] (reproduced from Wiley-VCH Verlag GmbH & Co. KGaA with permission) and (b) liposome coated LDH[109] (reproduced from Elsevier with permission).

brain tumor cells, and increased the delivery efficacy of 5-FU for effective inhibition of neural U87 and N2a cells.

In addition to the above surface coating method which is mostly *via* electrostatic attraction, another approach is to modify LDH nanoparticles through covalent bonding by making use of the –OH functional groups on the surface. Park *et al.* introduced (3-aminopropyl)triethoxysilane (APTES) to tailor LDH nanoparticles through condensation between the hydroxyl groups of LDH and the ethoxy groups of APTES molecules to form a covalent bond.[113] With this method, amine groups were grafted on the surface and interlayer spacing of LDH nanoparticles, making it convenient to attach other guest molecules. For example, the cancer cell specific ligand folic acid and fluorescein-5-isothiocyanate (FITC) were successfully conjugated onto the surface

 This journal is © The Royal Society of Chemistry 2019

Open Access Article. Published on 29 August 2019. Downloaded on 2/10/2026 5:01:13 AM.
This article is licensed under a Creative Commons Attribution 3.0 Unported Licence.

of amine-modified LDH nanoparticles through connection with amine functional groups.[114] Folic acid conjugated LDH nanoparticles showed greatly enhanced selectivity to folate receptor over-expressing cells (KB cells).[114] Wei *et al.* incorporated a near-infrared (NIR) dye into amine-modified LDH nanoparticles by electrostatic attraction, and further coated them with chitosan using glutaraldehyde as a cross-linking agent. These chitosan coated LDH nanoparticles had minimal cytotoxicity.[115] The subsequent *in vivo* application demonstrated the potential application of chitosan coated LDH nanoparticles for imaging.[115] Covalent conjugation of Cy5.5 molecules and Polyethylene glycol (PEG)-5000 to amine modified LDH nanoparticles was also reported, and LDH-PEG-5000 showed an enhanced blood circulation time without high fluorescence intensity in the major organs.[116] Yan *et al.* developed an approach to exfoliate LDH nanoparticles to thin individual layers so that it is possible to modify both sides of hydroxide nanosheets which are much thinner than conventional LDH nanoparticles. These exfoliated LDH thin layers could be linked with APTES-folic acid and these nanostructures were able to self-assemble into nanoclusters.[117,118] Through this approach, folic acid modified LDH nanoparticles were prepared for targeting cancer cells with folate receptor overexpression. Folic acid modified LDH nanoparticles possessed a high drug loading capacity of 27 wt% and dramatically improved the therapeutic efficacy of MTX.[117] A similar approach was also used to modify LDH nanoparticles with fluorescein molecules.[118] Attractively, this method produced LDH-fluorescein nanoparticles with a very high quantum yield (QY) of 55.1%. This is significantly better than those prepared through the previously reported anion exchange (3.0%) and coprecipitation (12.4%) approaches. Moreover, this type of LDH-fluorescein nanoparticles showed strong fluorescence even in a solid state, while conventional dye molecules completely lost fluorescence in a dry form due to concentration quenching. These nanostructures were also capable of self-assembling into a transparent, free-standing and fluorescent film.[118] Recently, Park *et al.* reported biodegradable LDH nanoparticles for active tumor targeting in siRNA transportation. In this work, folic acid conjugated LDH nanoparticles showed 3.0-fold higher suppression of tumor volume than the non-modified LDH system[119] (Fig. 10). Consistent with the improved siRNA delivery, a low level of Survivin protein and proliferating cell nuclear antigen (PCNA) in tumors was detected in the LDH-folic acid treated group. The results revealed that folic acid modified LDH nanoparticles loaded with siRNA efficiently suppressed Survivin expression at both post-transcriptional and translational levels and induced necrosis in cancer cells.

Recently, it was reported that photosensitizer Ce6 could be covalently conjugated to PEG modified LDH nanoflakes.[120] In this study, Ce6 molecules were firmly anchored to the stabilized LDH nanoflakes and showed very slow release profiles of Ce6, avoiding premature release of drug molecules in blood and ensuring their efficient delivery to tumors. It was found that LDH nanoparticles–Ce6 significantly inhibited tumor growth as indicated by the size reduction to 13.4%, 14.3% and 26.9% of the tumor volume in the PBS, LDH–Ce6 Mix, and free Ce6 treated groups, respectively. In addition, LDH could be exfoliated to ultrathin nanosheets with a size of 50 nm and a thickness of about 1.4–4 nm.[121] The fabricated nanosheets were tested for delivery of a negatively charged anticancer drug, MTX, in a mouse model, which demonstrated dramatically improved therapeutic efficacy, indicated by the effective inhibition of tumor growth with minimal side-effects. In comparison, if using the conventional non-surface modified LDH nanoparticles for delivery of MTX, the tumor inhibition efficacy is similar to that of free MTX molecules. Also importantly, with covalent conjugation, LDH nanostructures can not only load negatively charged species like conventional LDH nanoparticles, but also neutral molecules such as PEG and positively charged rhodamine B dyes.

4. LDH nanocomposites for biomedical applications

With the rapid development of LDH nanostructures, extensive research has also been extended to incorporating them with a spectrum of other materials to further broaden their applications. LDH based nanocomposites possess not only advantages and merits of LDH but also those of the combined materials. Therefore, the composites have the potential to satisfy advanced requirements of many practical utilizations.[122] Next, the biomedical and healthcare applications of LDH nanocomposites will be summarized.

4.1 Nanocomposites with LDH as the core

Silica coating is one of the most commonly used methods to coat nanoparticles because of its ease of further functionalization, optical transparency, good hydrophilicity, excellent stability and high biocompatibility.[123–128] Therefore, LDH nanoparticles were also decorated with a silica shell, using tetraethyl orthosilicate $Si(OC_2H_5)_4$ (TEOS) as a silica source.[122] Initially, a surfactant template method was reported for an efficient synthesis of an LDH@SiO_2 nanocomposite (Fig. 11a). In the method, CTAB was used as a surfactant-template to fabricate the LDH@SiO_2 nanocomposite. The obtained nanostructures had uniform and accessible mesopores ($\sim$2.2 nm), high surface area ($\sim$430 $m^2\ g^{-1}$), and large pore volume ($\sim$0.22 $cm^3\ g^{-1}$). This nanocomposite was tested for a slow release of ibuprofen.[129] Then surfactants FC4 and F127 were also introduced to synthesize the LDH@SiO_2 nanocomposite for sustained and pH sensitive release[130] (Fig. 11b). Li *et al.* used well-dispersed amine-functionalized SiO_2 nanodots to coat LDH by electrostatic interaction followed by condensation of APTES[11] (Fig. 11c). These LDH-SiO_2 dot nanostructures were well dispersible in cell culture medium and PBS buffer, and could be used to effectively deliver siRNA into U2OS cells.[11] Besides silica coating, a Gd-doped LDH@Au nanocomposite was fabricated for drug delivery and diagnosis.[9] This nanocomposite system displayed high DOX loading capacity, and enabled a pH sensitive release profile of DOX. The Gd-doped LDH@Au nanocomposite was able to efficiently deliver DOX into cells, release DOX in the cytoplasm, and ultimately cause cancer cell death.[9] Meanwhile, with Gd and Au doping, this nanocomposite could be employed for *in vitro* Computed Tomography (CT) and T1-weighted MR imaging, with

Open Access Article. Published on 29 August 2019. Downloaded on 2/10/2026 5:01:13 AM.
This article is licensed under a Creative Commons Attribution 3.0 Unported Licence.

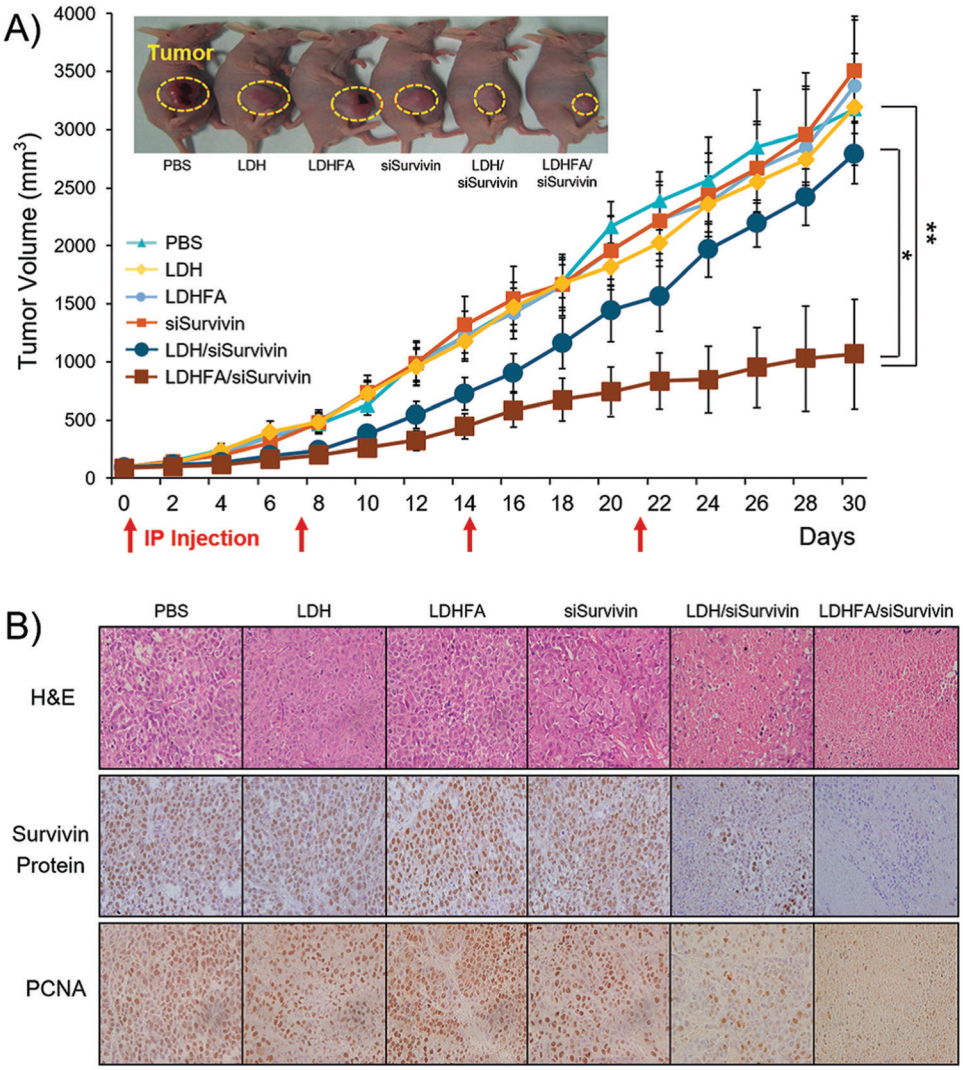

Fig. 10 *In vivo* anti-tumor effect and Survivin down-regulation in tumors treated with each sample through the IP route once every 7 days. (A) Tumor growth inhibition (n = 6 per group). Tumor volumes were measured at 2-day intervals. Tumor sizes are presented as means ± SE. *$p < 0.05$ *versus* LDH/siSurvivin treated group; ** $p < 0.01$ *versus* PBS-treated group (the inset shows the mice 18 days post-treatment. The tumor growth rate with LDHFA/siSurvivin was significantly slower, resulting in a tumor volume of 583 mm^3, which was remarkably smaller than the values in other groups: 1693 mm^3 (PBS); 1474 mm^3 (siSurvivin); 1157 mm^3 (LDH/siSurvivin)). (B) H&E, Survivin protein and PCNA stained tumor tissue section (n = 3 per group) (original magnification: ×100).[119] (Reproduced from Wiley-VCH Verlag GmbH & Co. KGaA with permission.)

a better performance than commercial MRI and CT contrast reagents and negligible cytotoxicity. A luminescent Eu-doped LDH nanocomposite was also synthesized with magnetic Fe_3O_4 nanoparticle coating.[131] This LDH could load 31% (w/w) ibuprofen and exhibited sustained release.[131]

4.2 Nanocomposites with LDH as the shell

A LDH based nanocomposite structure was designed using magnetic nanoparticles and LDH as the core and shell, respectively. This structure was fabricated with a simple one-step co-precipitation method.[132,133] Very attractively, it was explored that a greatly decreased drug release rate of diclofenac and ibuprofen was achieved when the composite structure was placed under a magnetic field. This magnetic field controlled "on–off" phenomenon is due to the instant aggregation of the magnetic nanocomposite induced by an external magnetic field.[132,133] This structure was then continued to be developed for cancer therapy.[134,135] In one representative study, the anticancer agent doxifluridine was loaded to monodispersed strongly magnetic Fe_3O_4@LDH nanostructures. This Fe_3O_4@LDH nanocomposite had a well-defined core–shell structure, strong magnetization and magnetic guided controlled release properties.[123] For drug delivery, carboxyl group modified DOX was loaded to the LDH shell *via* anion-exchange[135] (Fig. 12). This DOX-COOH loaded nanocomposite exhibited high cytotoxicity and powerful inhibition towards cancer cells (HeLa cells), but had low toxicity to normal cells (HEK 293T Cells). The mechanism may be explained as follows: the acidic cytoplasm of HeLa cells stimulated rapid degradation of the LDH shell and converted DOX-COOH to positively charged DOX, thereby rapidly escaping from the positively

 This journal is © The Royal Society of Chemistry 2019

Open Access Article. Published on 29 August 2019. Downloaded on 2/10/2026 5:01:13 AM.
This article is licensed under a Creative Commons Attribution 3.0 Unported Licence.

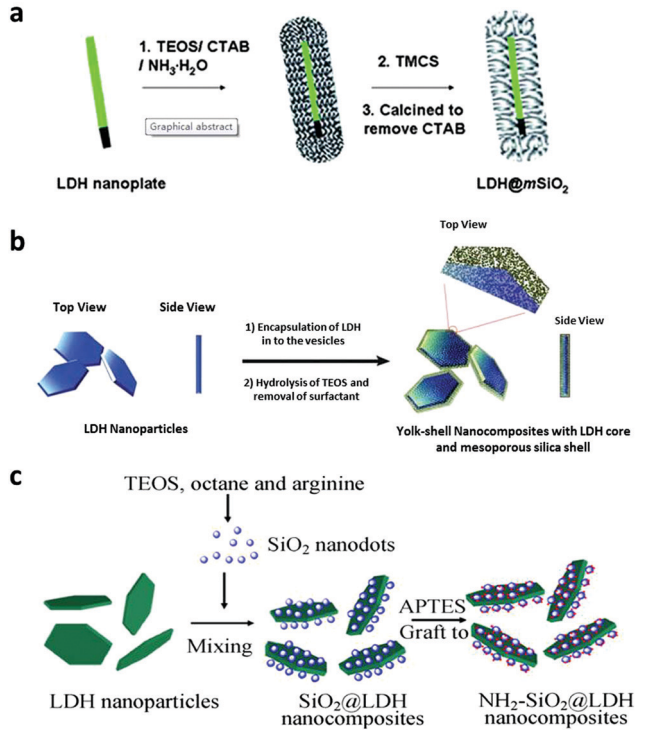

Fig. 11 Schematic illustration of the preparation of LDH core and silica shell nanocomposites[11,129,130] (reproduced from The Royal Society of Chemistry and Springer with permission).

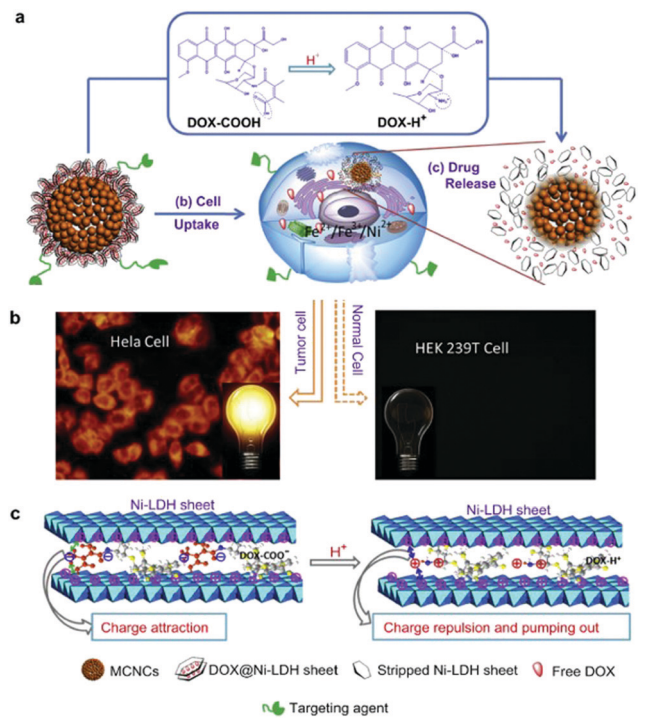

Fig. 12 (a) The plausible DOX release mechanism of DOX@MSPs/Ni-LDH-folate in the cytoplasm of tumor cells (acidic environment). (b) The different fluorescence behaviors of HeLa and HEK 293T cells incubated with nano-drugs. (c) The mechanism of pumping positively charged DOX out of the LDH sheets.[135] (reproduced from Elsevier with permission).

charged intercalation of the LDH shell by strong repulsive interaction, but the relatively neutral cytoplasm of HEK 293T cells caused a smaller amount of DOX to be released.[135] In addition to anticancer therapy, this type of magnetic nanoparticles@LDH nanocomposite was also used for separation of proteins.[136] Nanostructures with a SiO_2-coated Fe_3O_4 magnetite core and a LDH shell were synthesized by an *in situ* growth method (Fig. 13a). The as-fabricated nanocomposite was 600 nm in diameter, and had a large surface area (83 m^2 g^{-1}) and uniform mesochannels (4.3 nm) (Fig. 13b and c). The nanocomposite effectively and selectively separated histidine-tagged green fluorescent protein with a binding capacity of 239 μg mg^{-1}, and remained stable in several separation cycles[136] (Fig. 13d).

SiO_2 nanostructures were also encapsulated with a LDH shell. A 210 nm SiO_2@LDH core–shell nanocomposite was designed to enhance the immune adjuvant activity.[137] The zeta potential of this core–shell structure was 0.521 mV, making it easier for DNA binding compared with naked SiO_2 nanostructures which were negatively charged. The larger surface area of this nanocomposite can load a relatively large amount of DNA vaccine. Moreover, the SiO_2@LDH nanocomposite protected DNA from degradation, increased transfection efficiency, and efficiently promoted macrophage activation, compared with SiO_2 and LDH

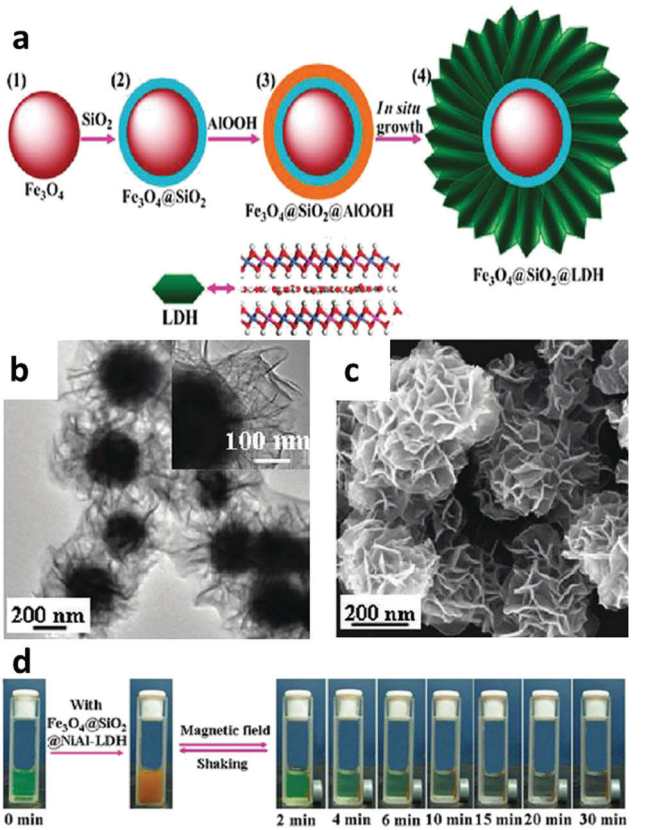

Fig. 13 (a) Schematic illustration of the fabrication of the Fe_3O_4@SiO_2@LDH nanocomposite; (b and c) TEM (b) and SEM (c) images of the Fe_3O4@SiO_2@NiAl-LDH nanocomposite; (d) photographs of separation of His-tagged GFP by Fe_3O_4@SiO_2@NiAl-LDH microspheres after different times[136] (reproduced from American Chemical Society with permission).

Open Access Article. Published on 29 August 2019. Downloaded on 2/10/2026 5:01:13 AM.
This article is licensed under a Creative Commons Attribution 3.0 Unported Licence.

alone.[137] The *in vivo* immunization study showed that this kind of DNA vaccine loaded SiO_2@LDH nanocomposite induced higher serum antibody response and also promoted T-cell proliferation and skewed T helper cells toward Th1 polarization.[137] Later on, a similar structure of SiO_2@LDH nanocomposite was used to deliver Newcastle disease virus DNA vaccine.[138] The composite structure possessed a great loading capacity of 39.66%, and led to increased *in vitro* gene transfection efficacy, and strong cellular, humoral and mucosal immune responses by intranasal immunization of specific pathogen-free chickens.[138] Additionally, the SiO_2@LDH nanocomposite was designed for controlled release. Mesoporous silica was used as a core material to load guest molecules of ($Ru(bpy)_3Cl_2$) followed by encapsulation of LDH nanosheets *via* electrostatic adsorption[139] (Fig. 14). This nanocomposite was used for pH-responsive controlled release by dissolution of the LDH coating in an acidic environment to trigger the release of the drug from mesoporous silica nanoparticles: almost no ($Ru(bpy)_3Cl_2$) release was found from the SiO_2@LDH nanocomposite in the physiological environment (pH = 7.4), while slow and fast release took place at pH = 4.0/5.0 and pH = 3.0, respectively (Fig. 14a). Moreover, a multifunctional Y_2O_3:Er^{3+},Yb^{3+}@SiO_2@LDH nanocomposite system was fabricated for simultaneous tumor optical imaging and therapy.[140] LDH nanosheets were deposited on the surface of monodispersed SiO_2 coated Y_2O_3:Er^{3+},Yb^{3+} nanoparticles by precipitation followed by hydrothermal treatment.[140] In this system, Y_2O_3:Er^{3+},Yb^{3+} nanoparticles worked as a near infrared fluorescent nanophosphor which exhibited strong red upconversion fluorescence under 980 nm laser irradiation. The positively charged surface of LDH was utilized as an anticancer drug nanovehicle for efficient intracellular delivery.[140]

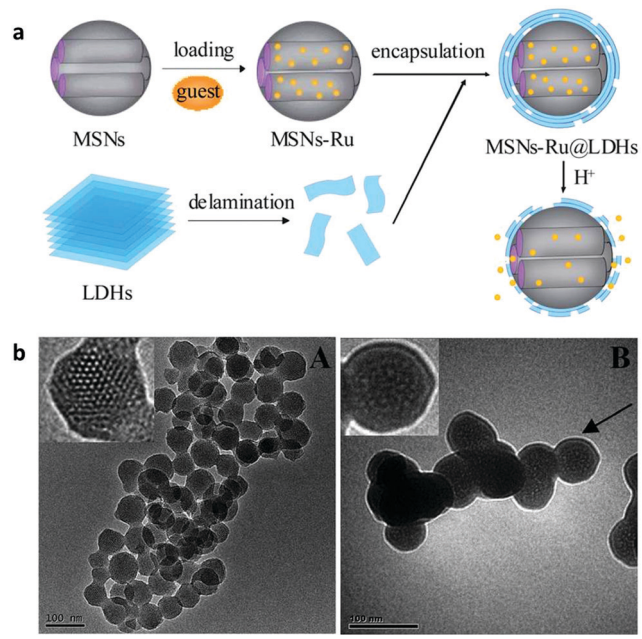

Fig. 14 (a) Synthesis procedure of MSN–Ru@LDH and the pH-responsive controlled release mechanism; (b) TEM images of (A) MSNs and (B) MSN–Ru@LDH (MSN–Ru: $Ru(bpy)_3^{2+}$ loaded mesoporous silica nanoparticles).[139] (Reproduced from Royal Society of Chemistry with permission.)

Au nanoparticles have also been employed as a core material, wrapped with LDH. In this work, MTX was first attached to citrate-stabilized Au nanoparticles; then, a SiO_2 layer was decorated on the surface of the Au nanostructure using tetraethyl orthosilicate (TEOS) as a silica source; later, NaOH was added to the SiO_2 shell; and finally, Mg^{2+} and Al^{3+} were added to the solution to obtain a LDH shell.[141] By controlling the pH of SiO_2 etching, a core/shell structure (pH 11) or a york/shell structure (pH 10.5) was able to be controllably synthesized. MTX loaded to this nanostructure exhibited better anticancer efficiency, compared with free MTX and LDH-MTX.

4.3 LDH thin film coating

LDH based film coating has been widely used for antimicrobial, sensing, electrochemical and optical applications.[142–148] In a typical work, substrates including metals, ceramics, and glass were coated with oriented LDH films with strong adhesion. Subsequently, silver ions were *in situ* reduced to metallic silver nanoparticles and evenly distributed on the LDH surface[149] (Fig. 15a and b). The Ag-LDH coating showed excellent and durable antimicrobial activities against both Gram-negative (*E. coli* and *P. aeruginosa*) and Gram-positive (*B. subtilis* and *S. aureus*) bacteria[149] (Fig. 15c–g). Ciprofloxacin loaded LDH was also coated on a middle ear prostheses implant to combat

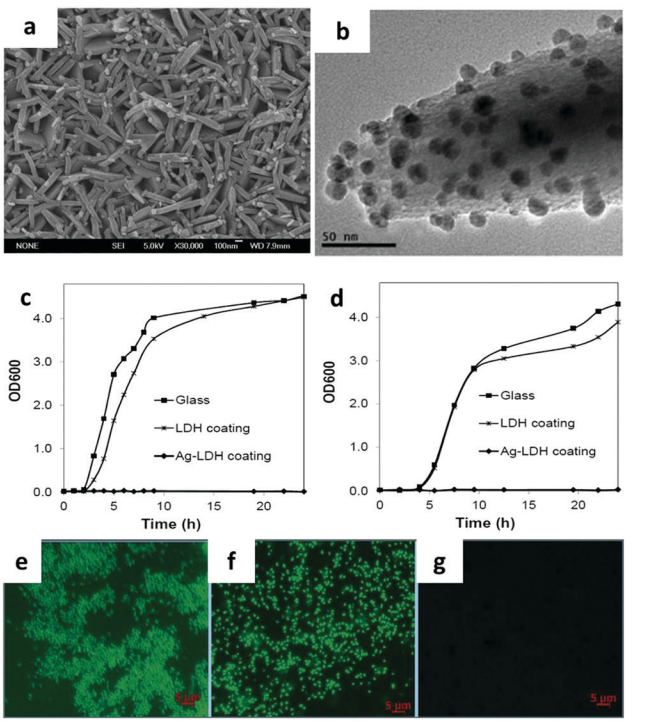

Fig. 15 (a) SEM image of Ag-LDH, (b) TEM image of Ag-LDH coating scraped from the substrate. (c and d) Bacterial growth curves of (c) *E. coli* and (d) *B. subtilis* in Luria-Bertani broth in the presence of the glass substrate, LDH coating and Ag-LDH coating on the glass substrates. (e–g) Confocal microscopy images of *E. coli* on the surface of (e) glass, (f) LDH coating, and (g) Ag-LDH coating after 24 h of culture (live cells stained green).[149] (Reproduced from Wiley-VCH Verlag GmbH & Co. KGaA with permission.)

This journal is © The Royal Society of Chemistry 2019

Open Access Article. Published on 29 August 2019. Downloaded on 2/10/2026 5:01:13 AM.
This article is licensed under a Creative Commons Attribution 3.0 Unported Licence.

infection with *P. aeruginosa*.[150] The film displayed excellent activity against infection immediately after implantation, also with persisting attenuated activity when re-infection was triggered at 1 week after surgery.[150] Similar techniques were as well applied to decorate porous titanium implants with antibiotics for prolonged antibiotic release, improved cell adhesion and good *in vitro* and *in vivo* antibacterial effects.[151] It was found that middle ear prostheses coated with LDH showed little signs of degradation after being implanted into the middle ear of rabbits for 10 days, indicating that the LDH has excellent biocompatibility and stability in the middle ear.[152] Moreover, Peng *et al.* reported Mg–Al LDH and $Mg(OH)_2$ co-coated Mg–Nd–Zn–Zr alloy to improve its corrosion resistance and biocompatibility.[153] The LDH coated alloy also showed greatly enhanced cell adhesion, migration and proliferation and a decreased hemolysis ratio to a level suitable for clinical application. The *in vivo* study demonstrated that the $Mg(OH)_2$ and Mg–Al LDH coating exhibited better histocompatibility than pure $Mg(OH)_2$ coatings or untreated magnesium alloy.

4.4 Other types of LDH based composites

As a ceramic material, LDH has superior mechanical, optical and thermal properties which pure polymers normally lack.[154–157] Taking advantage of these merits, LDH nanoparticles can be regarded as a filler to incorporate into the polymer matrix to form nanocomposites and thus improve the desirable property of a pure polymer matrix.[158–162] In one application, LDH nanoparticles were added to carboxymethylcellulose (CMC) to fabricate mechanically strengthened dissolvable polymer microneedles for improved transdermal delivery to human skin.[163] The addition of LDH nanoparticles dramatically improved the mechanical property of weak dissolving polymers: the elastic modulus of CMC was measured to be 0.993 ± 0.065 and 2.878 ± 0.123 GPa before and after the addition of 5 wt% LDH to CMC (Fig. 16a). With the improved mechanical strength, LDH-CMC microneedles could penetrate pig and human skin much more uniformly, also with a substantially greater penetration depth than CMC microneedles (Fig. 16b and c). The advantage of this mechanically strengthened LDH-CMC nanocomposite is that it still dissolves very rapidly within the skin (Fig. 16d and e), while previously reported mechanically strengthened microneedles suffer from slower dissolution rates, which can affect their clinical use as dissolvable microneedles.[163–165]

In addition, Mg–Al LDH nanoparticles were added to chitosan to fabricate a porous scaffold and loaded with Pifithrin-α (PFTα) to enhance stem cell osteogenic differentiation and bone regeneration.[166] PFTα molecules exhibit a potent ability to induce osteogenesis of hBMSCs *via* the GSK3β/β-catenin pathway. Here the LDH-CS-PFTα scaffold was demonstrated to significantly enhance the osteogenic differentiation of hBMSCs. When used in an *in vivo* test, the scaffold greatly increased the repair and regeneration of bone tissue in cranial defect model rats in comparison with that in the control rats at 12 weeks post-implantation. Thus, the development of a LDH-chitosan based scaffold provided a promising strategy for tissue engineering applications. Recently, a bone remodeling drug, risedronate (RS), was loaded into LDH nanoparticles, followed by the formation of a sheet with poly(lactic-*co*-glycolic acid) on a clinically approved bioabsorbable bone plate (Fig. 17).[167] In this design, the presence of metals in LDH enabled *in vivo* X-ray images for up to 4 weeks after implantation. In the meantime, the sustained release of drug greatly improved bone regeneration.[167]

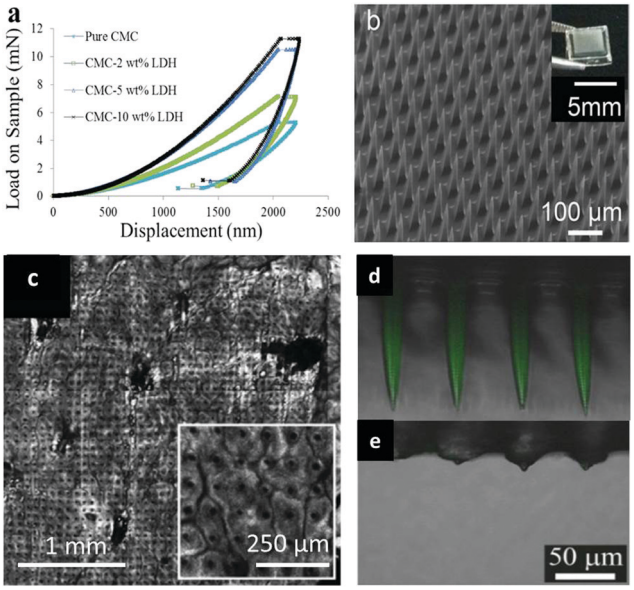

Fig. 16 (a) Load–displacement curves of pure sodium carboxymethylcellulose (CMC) and CMC with LDH fillers; (b) fabricated dissolving polymer microneedles (inset: digital camera image of a polymer microneedle array); (c) reflectance confocal microscopy images of pig skin after 5 min CMC–LDH nanocomposite microneedle application; (d and e) merged fluorescence and reflectance confocal microscopy images of CMC–LDH nanocomposite microneedles: (d) before application and (e) 5 min after application to pig skin.[163] (Reproduced from Wiley-VCH Verlag GmbH & Co. KGaA with permission).

5. Discussion

5.1 Advantages of LDH nanostructures

LDH nanostructures have been extensively studied for about 20 years with constantly increasing interest as indicated in the introduction. For biomedical applications, LDH nanostructures offer many advantages. First, these nanostructures possess pH sensitivity. LDH nanostructures are made of hydroxides, making them sensitive to acidic environments with very good biodegradability. This enables LDH nanostructures to be ideal for cancer therapy as tumor tissues and cancer cells possess lower pH. Using pH as a stimuli has constantly been a popular strategy for controlled drug delivery and release. Biodegradability is also very important for body clearance of the material and consequently for enhancing biocompatibility and safety profile.[168] Second, the metal component of LDH nanostructures could be easily tuned for different applications.[169–171] For the consideration of biocompatibility, metal ions like Zn^{2+}, Mg^{2+} and Al^{3+} are the typical candidates for divalent and trivalent metal cations, respectively. Other types of metal ions like Mn^{2+} can also

Open Access Article. Published on 29 August 2019. Downloaded on 2/10/2026 5:01:13 AM.
This article is licensed under a Creative Commons Attribution 3.0 Unported Licence.

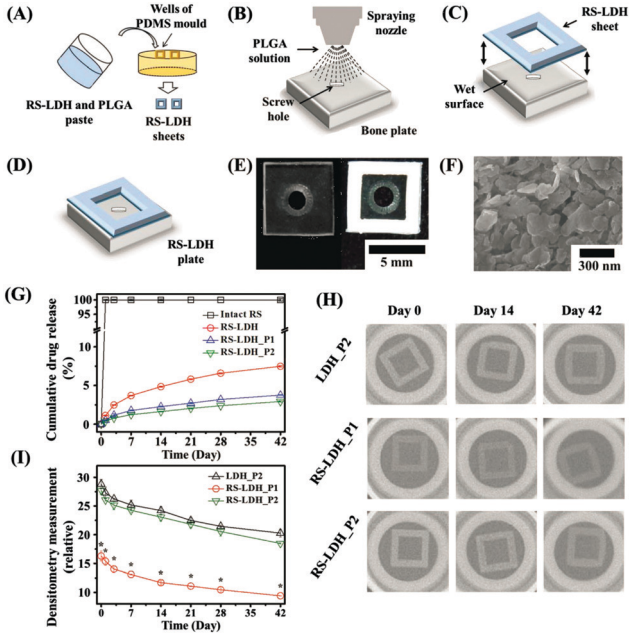

Fig. 17 Schematic preparation process of a theranostic plate. (A) RS-LDH sheets were separately prepared using polydimethylsiloxane (PDMS) molds consisting of square-shaped frames filled with a paste of RS-LDH and PLGA (5 : 1, w/w). (B) PLGA solution was sprayed onto the surface of a bone plate, and (C) the RS-LDH sheet was attached to the top to produce (D) the theranostic bone plate. (E) Optical images of the bioabsorbable bone fixation plates with and without a theranostic RS-LDH sheet. (F) FE-SEM image of the surface of a theranostic RS-LDH sheet. (G) *In vitro* drug-release profiles of the intact RS, RS-LDH, RS-LDH_P1, and RS-LDH_P2 in PBS (pH 7.4). (H) Representative *in vitro* X-ray images and (I) densitometry measurements of LDH_P2, RS-LDH_P1, and RS-LDH_P2 over 42 d. *RS-LDH_P1 differs significantly from both LDH_P2 and RS-LDH_P2 ($p < 0.05$).[167] (Reproduced from Wiley-VCH Verlag GmbH & Co. KGaA with permission.)

be incorporated for MRI observation. Compared with other materials such as semiconductor quantum dots for fluorescence imaging, MRI is much more clinically relevant.[172] Third, LDH nanostructures are competent for cell membrane penetration due to their positive charge, thereby greatly improving intracellular delivery efficacy. Biological barriers are the major obstacles of effective delivery of drugs, genes and biomolecules into the cell cytoplasm.[173,174] Fourth, the drug loading process can be very straightforward in the case of negatively charged species and the drug loading capacity is relatively high. Fifth, the fabrication is cheap and the size tunability can vary with a wide range from 20 nm to 10 μm, suitable for different biological and clinical applications. This size tunability is far greater than for most other types of nanomaterials. Sixth, our research showed that ultra-thin LDH nanosheets tend to preferably accumulate in the kidney instead of liver like most other nanomaterials.[121] This may be good for subsequent clearance and more suitable for clinical applications.[175,176] Seventh, LDH has a great flexibility to form numerous types of composites for various utilizations. Furthermore, LDH is a type of ceramic nanoparticles with very high mechanical strength and therefore can be utilized as a filler to modify the mechanical strength of a polymer matrix for specific applications and also as a thin film coating on various kinds of implantation devices.

5.2 Challenges of LDH nanostructures for biomedical applications

Although LDH nanostructures possess superior advantages that seem very promising for future applications, several challenges are still remaining. For example, because of the positive charge of LDH nanostructures, they may interact with negatively charge biomolecules in the biological environment and lead to loss of surface charge and aggregation. This challenge becomes crucial when LDH nanostructures are administrated *via* the blood system. Therefore, improvement of the stability of LDH nanostructures is a major challenge. Second, compared with other nanomaterials, there is less flexibility in functionalizing the surface of LDH nanostructures. For conventional LDH nanoparticles, due to the bulky thickness, the surface modification of the 2 outermost LDH layers is not enough for high stability in the biological environment. Therefore, it is important to develop new generations of ultra-thin LDH nanosheets with flexibility of surface modification for practical applications. Third, in comparison with other inorganic materials such as silica and gold nanoparticles, the controllability of the fabrication of LDH nanostructures and the reproducibility need to be substantially improved. To tackle this issue, continuous synthesis has been employed instead of the traditional flow chemistry approaches that allow reducing the residence time and maintaining almost constant supersaturation to produce LDH in large amounts.[177]

6. Conclusions and future outlook

This review summarizes the development of LDH nanomaterials including pristine LDH nanostructures, surface modified LDH nanostructures, and LDH based nanocomposites for biomedical applications. LDH shows good biocompatibility, pH sensitivity, biodegradability, high intracellular delivery efficacy, and great flexibility in size tunability and nanocomposite formation. Initially, pristine LDH nanostructures were used for drug and gene delivery and photodynamic therapy. Although effective, it is desirable to surface modify these LDH nanostructures for improved properties due to the importance of the surface of nanomaterials. Surface modification not only makes LDH nanostructures more stable in buffer solution and blood system, but also enables versatile functions such as targeted delivery. Beyond using LDH nanostructures alone, there is great flexibility to combine LDH with many other materials such as metals, metal oxides, and polymers to further extend their functions and applications. It is expected that LDH nanomaterials have great potential in clinical applications due to their unique characteristics. In the future, the following aspects need to be explored to facilitate the application of LDH nanomaterials and their potential commercial use in the clinic. Firstly, it is essential to improve the synthesis approaches to produce highly uniform and reproducible LDH nanostructures with small variation in size, thickness, and geometry. Secondly, surface modification and drug loading under mild conditions

 This journal is © The Royal Society of Chemistry 2019

Open Access Article. Published on 29 August 2019. Downloaded on 2/10/2026 5:01:13 AM.
This article is licensed under a Creative Commons Attribution 3.0 Unported Licence.

need to be established to ensure improved properties and minimize the influence of drug loading conditions such as temperature, time and pH on loaded drugs and genes. Thirdly, it is required to fabricate highly stable LDH nanomaterials in biological solution so that the drug delivery system can efficiently transport drugs and genes to target sites with minimal pre-mature drug and gene release. The high stability will prevent aggregation of nanostructures which can result in low therapeutic efficacy and possible precipitation in blood circulation. In this regard, it is desirable to develop ultra-thin LDH nanosheets. Fourthly, it is needed to thoroughly understand the *in vivo* biodegradability, biodistribution, and clearance of LDH nanomaterials. Fifthly, the flexibility of formation of LDH nanocomposites is an important advantage of LDH. This area of research should be significantly expanded, particularly by combining with materials which can circumvent the limitation of LDH nanostructures or enhance properties and performance. Moreover, there are many other types of nanostructures for biomedical applications such as bioceramic nanoparticles. However, there is a lack of studies that compare different types of nanomaterials with the same standard protocols for direct comparison so it is difficult to identify the best candidate for practical applications.

Conflicts of interest

There are no conflicts.

Acknowledgements

This work was financially supported by the General Research Fund of Hong Kong (GRF CityU Grant No. 11306717 and 11338516).

References

1 Z. P. Xu, G. Stevenson, C. Q. Lu and G. Q. Lu, *J. Phys. Chem. B*, 2006, **110**, 16923–16929.
2 Z. P. Xu, G. S. Stevenson, C. Q. Lu, G. Q. Lu, P. F. Bartlett and P. P. Gray, *J. Am. Chem. Soc.*, 2006, **128**, 36–37.
3 P. J. Sideris, U. G. Nielsen, Z. Gan and C. P. Grey, *Science*, 2008, **321**, 113–117.
4 Q. Wang and D. O'Hare, *Chem. Rev.*, 2012, **112**, 4124–4155.
5 L. Sheng, J. Y. Liu, C. Zhang, L. P. Zou, Y. Y. Li and Z. P. Xu, *Bioresour. Technol.*, 2019, **271**, 190–195.
6 R. J. Wang, W. J. Zhang, G. H. He and P. Gao, *J. Mater. Chem. A*, 2014, **2**, 16416–16423.
7 F. Song and X. L. Hu, *Nat. Commun.*, 2014, **5**, 4477.
8 M. Shao, F. Ning, J. Zhao, M. Wei, D. G. Evans and X. Duan, *J. Am. Chem. Soc.*, 2012, **134**, 1071–1077.
9 L. Wang, H. Xing, S. Zhang, Q. Ren, L. Pan, K. Zhang, W. Bu, X. Zheng, L. Zhou, W. Peng, Y. Hua and J. Shi, *Biomaterials*, 2013, **34**, 3390–3401.
10 J. C. Sun, J. J. Li, H. Fan and S. Y. Ai, *J. Mater. Chem. B*, 2013, **1**, 5436–5442.
11 L. Li, W. Y. Gu, J. Liu, S. Y. Yan and Z. P. Xu, *Nano Res.*, 2015, **8**, 682–694.
12 L. Yan, J. F. Zhang, C. S. Lee and X. F. Chen, *Small*, 2014, **10**, 4487–4504.
13 M. Elsabahy and K. L. Wooley, *Chem. Soc. Rev.*, 2012, **41**, 2545–2561.
14 E. Blanco, H. Shen and M. Ferrari, *Nat. Biotechnol.*, 2015, **33**, 941–951.
15 Y. Chen and L. Liu, *Adv. Drug Delivery Rev.*, 2012, **64**, 640–665.
16 Y. Wang, M. S. Shim, N. S. Levinson, H. W. Sung and Y. Xia, *Adv. Funct. Mater.*, 2014, **24**, 4206–4220.
17 L. Yan, Y. Yang, W. J. Zhang and X. F. Chen, *Adv. Mater.*, 2014, **26**, 5533–5540.
18 A. M. Wen and N. F. Steinmetz, *Chem. Soc. Rev.*, 2016, **45**, 4074–4126.
19 K. S. Sunderland, M. Yang and C. Mao, *Angew. Chem., Int. Ed.*, 2017, **56**, 1964–1992.
20 A. E. Czapar, Y. R. Zheng, I. A. Riddell, S. Shukla, S. G. Awuah, S. J. Lippard and N. F. Steinmetz, *ACS Nano*, 2016, **10**, 4119–4126.
21 S. J. Tseng, K. Y. Huang, I. M. Kempson, S. H. Kao, M. C. Liu, S. C. Yang, Z. X. Liao and P. C. Yang, *ACS Nano*, 2016, **10**, 10339–10346.
22 M. A. Kay, J. C. Glorioso and L. Naldini, *Nat. Med.*, 2001, **7**, 33–40.
23 D. W. Pack, A. S. Hoffman, S. Pun and P. S. Stayton, *Nat. Rev. Drug Discovery*, 2005, **4**, 581–593.
24 B. Gupta, T. S. Levchenko and V. P. Torchilin, *Adv. Drug Delivery Rev.*, 2005, **57**, 637–651.
25 S. Mura, J. Nicolas and P. Couvreur, *Nat. Mater.*, 2013, **12**, 991–1003.
26 N. M. Idris, M. K. Gnanasammandhan, J. Zhang, P. C. Ho, R. Mahendran and Y. Zhang, *Nat. Med.*, 2012, **18**, 1580–1585.
27 Z. J. Zhang, L. M. Wang, J. Wang, X. M. Jiang, X. H. Li, Z. J. Hu, Y. H. Ji, X. C. Wu and C. Y. Chen, *Adv. Mater.*, 2012, **24**, 1418–1423.
28 X. F. Chen and W. J. Zhang, *Chem. Soc. Rev.*, 2017, **46**, 734–760.
29 C. Chiappini, E. De Rosa, J. O. Martinez, X. Liu, J. Steele, M. M. Stevens and E. Tasciotti, *Nat. Mater.*, 2015, **14**, 532–539.
30 Y. Wang, Y. Yang, L. Yan, S. Y. Kwok, W. Li, Z. G. Wang, X. Y. Zhu, G. Y. Zhu, W. J. Zhang, X. F. Chen and P. Shi, *Nat. Commun.*, 2014, **5**, 4466.
31 E. Y. W. Chong, C. Y. P. Ng, V. W. Y. Choi, L. Yan, Y. Yang, W. J. Zhang, K. W. K. Yeung, X. F. Chen and K. N. Yu, *J. Mater. Chem. B*, 2013, **1**, 3390–3396.
32 X. F. Chen, G. Y. Zhu, Y. Yang, B. L. Wang, L. Yan, K. Y. Zhang, K. K. W. Lo and W. J. Zhang, *Adv. Healthcare Mater.*, 2013, **2**, 1103–1107.
33 X. Y. Zhu, M. F. Yuen, L. Yan, Z. Y. Zhang, F. J. Ai, Y. Yang, P. K. N. Yu, G. Y. Zhu, W. J. Zhang and X. F. Chen, *Adv. Healthcare Mater.*, 2016, **5**, 1157–1168.
34 Y. Chen, C. L. Tan, H. Zhang and L. Z. Wang, *Chem. Soc. Rev.*, 2015, **44**, 2681–2701.
35 Y. Zhang, B. Y. W. Hsu, C. L. Ren, X. Li and J. Wang, *Chem. Soc. Rev.*, 2015, **44**, 315–335.

Open Access Article. Published on 29 August 2019. Downloaded on 2/10/2026 5:01:13 AM.
This article is licensed under a Creative Commons Attribution 3.0 Unported Licence.

36 P. P. Yang, S. L. Gai and J. Lin, *Chem. Soc. Rev.*, 2012, **41**, 3679–3698.
37 M. Zhang, Y. H. Zhao, L. Yan, R. Peltier, W. L. Hui, X. Yao, Y. L. Cui, X. F. Chen, H. Y. Sun and Z. K. Wang, *ACS Appl. Mater. Interfaces*, 2016, **8**, 8834–8840.
38 K. Yang, L. Z. Feng, X. Z. Shi and Z. Liu, *Chem. Soc. Rev.*, 2013, **42**, 530–547.
39 L. Liu, Y. H. Tang, S. Dai, F. Kleitz and S. Z. Qiao, *Nanoscale*, 2016, **8**, 12803–12811.
40 J. F. Lin, J. Li, A. Gopal, T. Munshi, Y. W. Chu, J. X. Wang, T. T. Liu, B. Y. Shi, X. F. Chen and L. Yan, *Chem. Commun.*, 2019, **55**, 2656–2659.
41 X. Q. Chen, J. Sun, H. Zhao, K. Yang, Y. D. Zhu, H. R. Luo, K. Yu, H. S. Fan and X. D. Zhang, *J. Mater. Chem. B*, 2018, **6**, 3586–3599.
42 X. Q. Chen, Y. J. Tang, A. M. Liu, Y. D. Zhu, D. Gao, Y. Yang, J. Sun, H. S. Fan and X. D. Zhang, *ACS Appl. Mater. Interfaces*, 2018, **10**, 14378–14388.
43 H. Zhao, C. H. Wu, D. Gao, S. P. Chen, Y. D. Zhu, J. Sun, H. R. Luo, K. Yu, H. S. Fan and X. D. Zhang, *ACS Nano*, 2018, **12**, 7838–7854.
44 H. Zhao, S. P. Chen, Y. H. He, C. H. Wu, Y. D. Zhu, K. Yu and H. S. Fan, *Nanoscale*, 2018, **10**, 11624–11632.
45 M. Lan, S. Zhao, W. Liu, C. S. Lee, W. Zhang and P. Wang, *Adv. Healthcare Mater.*, 2019, e1900132, DOI: 10.1002/adhm.201900132.
46 M. Lan, J. Zhang, Y. S. Chui, P. Wang, X. Chen, C. S. Lee, H. L. Kwong and W. Zhang, *ACS Appl. Mater. Interfaces*, 2014, **6**, 21270–21278.
47 J. H. Choy, S. Y. Kwak, Y. J. Jeong and J. S. Park, *Angew. Chem., Int. Ed.*, 2000, **39**, 4042–4045.
48 J. H. Choy, J. S. Jung, J. M. Oh, M. Park, J. Jeong, Y. K. Kang and O. J. Han, *Biomaterials*, 2004, **25**, 3059–3064.
49 R. Ma, Z. G. Wang, L. Yan, X. F. Chen and G. Y. Zhu, *J. Mater. Chem. B*, 2014, **2**, 4868–4875.
50 G. Choi, O. J. Kwon, Y. Oh, C. O. Yun and J. H. Choy, *Sci. Rep.*, 2014, **4**, 4430.
51 R. Z. Liang, R. Tian, L. Ma, L. L. Zhang, Y. L. Hu, J. Wang, M. Wei, D. Yan, D. G. Evans and X. Duan, *Adv. Funct. Mater.*, 2014, **24**, 3144–3151.
52 X. Mei, S. M. Xu, T. Y. Hu, L. Q. Peng, R. Gao, R. Z. Liang, M. Wei, D. Evans and X. Duan, *Nano Res.*, 2018, **11**, 195–205.
53 R. Gao, X. Mei, D. P. Yan, R. Z. Liang and M. Wei, *Nat. Commun.*, 2018, **9**, 2798.
54 V. Rives, M. del Arco and C. Martin, *J. Controlled Release*, 2013, **169**, 28–39.
55 Z. Gu, A. C. Thomas, Z. P. Xu, J. H. Campbell and G. Q. Lu, *Chem. Mater.*, 2008, **20**, 3715–3722.
56 Z. Gu, B. E. Rolfe, Z. P. Xu, A. C. Thomas, J. H. Campbell and G. Q. Lu, *Biomaterials*, 2010, **31**, 5455–5462.
57 Z. Gu, B. E. Rolfe, A. C. Thomas, J. H. Campbell, G. Q. Lu and Z. P. Xu, *Biomaterials*, 2011, **32**, 7234–7240.
58 Z. Gu, B. E. Rolfe, Z. P. Xu, J. H. Campbell, G. Q. Lu and A. C. Thomas, *Adv. Healthcare Mater.*, 2012, **1**, 669–673.
59 S. Y. Yan, B. E. Rolfe, B. Zhang, Y. H. Mohammed, W. Y. Gu and Z. P. Xu, *Biomaterials*, 2014, **35**, 9508–9516.
60 W. Y. Chen, B. Zhang, T. Mahony, W. Y. Gu, B. Rolfe and Z. P. Xu, *Small*, 2016, **12**, 1627–1639.
61 L. L. Qin, W. R. Wang, S. H. You, J. M. Dong, Y. H. Zhou and J. B. Wang, *Int. J. Nanomed.*, 2014, **9**, 5701–5710.
62 W. R. Wang, A. Li, W. Mei, R. R. Zhu, K. Li, X. Y. Sun, Y. C. Qian and S. L. Wang, *RSC Adv.*, 2015, **5**, 23826–23834.
63 S. Y. Kwak, W. M. Kriven, M. A. Wallig and J. H. Choy, *Biomaterials*, 2004, **25**, 5995–6001.
64 Z. P. Xu, M. Niebert, K. Porazik, T. L. Walker, H. M. Cooper, A. P. J. Middelberg, P. P. Gray, P. F. Bartlett and G. Q. Lu, *J. Controlled Release*, 2008, **130**, 86–94.
65 S. Senapati, R. Thakur, S. P. Verma, S. Duggal, D. P. Mishra, P. Das, T. Shripathi, M. Kumar, D. Rana and P. Maiti, *J. Controlled Release*, 2016, **224**, 186–198.
66 L. Naldini, *Nature*, 2015, **526**, 351–360.
67 J. Kim, J. Kim, C. Jeong and W. J. Kim, *Adv. Drug Delivery Rev.*, 2016, **98**, 99–112.
68 L. Lambricht, A. Lopes, S. Kos, G. Sersa, V. Preat and G. Vandermeulen, *Expert Opin. Drug Delivery*, 2016, **13**, 295–310.
69 K. Chatterjee, J. W. Chiu, H. Yu, P. S. Loh, A. Ghosh and V. Patzel, *Mol. Ther.*, 2019, **27**, 233.
70 H. Yin, R. L. Kanasty, A. A. Eltoukhy, A. J. Vegas, J. R. Dorkin and D. G. Anderson, *Nat. Rev. Genet.*, 2014, **15**, 541–555.
71 X. Du, C. X. Zhao, M. Y. Zhou, T. Y. Ma, H. W. Huang, M. Jaroniec, X. J. Zhang and S. Z. Qiao, *Small*, 2017, **13**, 1602592.
72 L. Xiong, J. X. Bi, Y. H. Tang and S. Z. Qiao, *Small*, 2016, **12**, 4735–4742.
73 L. Xiong and S. Z. Qiao, *Nanoscale*, 2016, **8**, 17446–17450.
74 H. B. Xia, Q. W. Mao, H. L. Paulson and B. L. Davidson, *Nat. Biotechnol.*, 2002, **20**, 1006–1010.
75 M. Jimenez-Sanchez, W. Lam, M. Hannus, B. Sonnichsen, S. Imarisio, A. Fleming, A. Tarditi, F. Menzies, T. E. Dami, C. Xu, E. Gonzalez-Couto, G. Lazzeroni, F. Heitz, D. Diamanti, L. Massai, V. P. Satagopam, G. Marconi, C. Caramelli, A. Nencini, M. Andreini, G. L. Sardone, N. P. Caradonna, V. Porcari, C. Scali, R. Schneider, G. Pollio, C. J. O'Kane, A. Caricasole and D. C. Rubinsztein, *Nat. Chem. Biol.*, 2015, **11**, 347–354.
76 S. Prakash, M. Malhotra and V. Rengaswamy, *Methods Mol. Biol.*, 2010, **623**, 211–229.
77 M. E. Davis, J. E. Zuckerman, C. H. J. Choi, D. Seligson, A. Tolcher, C. A. Alabi, Y. Yen, J. D. Heidel and A. Ribas, *Nature*, 2010, **464**, 1067–1070.
78 H. M. Liu, C. M. Qiao, J. Yang, J. Weng and X. Zhang, *J. Mater. Chem. B*, 2014, **2**, 5910–5924.
79 P. Y. Teo, C. Yang, L. M. Whilding, A. C. Parente-Pereira, J. Maher, A. J. T. George, J. L. Hedrick, Y. Y. Yang and S. Ghaem-Maghami, *Adv. Healthcare Mater.*, 2015, **4**, 1180–1189.
80 L. Zhou, Y. W. Xi, M. Chen, W. Niu, M. Wang, P. X. Ma and B. Lei, *Nanoscale*, 2019, **11**, 4614.
81 E. Crouchet, R. Saad, C. Affolter-Zbaraszczuk, J. Ogier, T. F. Baumert, C. Schuster and F. Meyer, *J. Mater. Chem. B*, 2017, **5**, 858–865.

This journal is © The Royal Society of Chemistry 2019

Open Access Article. Published on 29 August 2019. Downloaded on 2/10/2026 5:01:13 AM. This article is licensed under a Creative Commons Attribution 3.0 Unported Licence.

82 L. Desigaux, M. Ben Belkacem, P. Richard, J. Cellier, P. Leone, L. Cario, F. Leroux, C. Taviot-Gueho and B. Pitard, *Nano Lett.*, 2006, **6**, 199–204.
83 S. D. Li, J. H. Li, C. J. Wang, Q. Wang, M. Z. Cader, J. Lu, D. G. Evans, X. Duan and D. O'Hare, *J. Mater. Chem. B*, 2013, **1**, 61–68.
84 Z. P. Xu, T. L. Walker, K. L. Liu, H. M. Cooper, G. Q. M. Lu and P. F. Bartlett, *Int. J. Nanomed.*, 2007, **2**, 163–174.
85 K. Ladewig, M. Niebert, Z. P. Xu, P. P. Gray and G. Q. M. Lu, *Biomaterials*, 2010, **31**, 1821–1829.
86 Y. Y. Wong, K. Markham, Z. P. Xu, M. Chen, G. Q. Lu, P. F. Bartlett and H. M. Cooper, *Biomaterials*, 2010, **31**, 8770–8779.
87 N. Mitter, E. A. Worrall, K. E. Robinson, P. Li, R. G. Jain, C. Taochy, S. J. Fletcher, B. J. Carroll, G. Q. Lu and Z. P. Xu, *Nat. Plants*, 2017, **3**, 16207.
88 J. A. Kemp, M. S. Shim, C. Y. Heo and Y. J. Kwon, *Adv. Drug Delivery Rev.*, 2016, **98**, 3–18.
89 D. Hughes and D. I. Andersson, *Nat. Rev. Genet.*, 2015, **16**, 459–471.
90 Y. Wen, W. Zhang, N. Q. Gong, Y. F. Wang, H. B. Guo, W. S. Guo, P. C. Wang and X. J. Liang, *Nanoscale*, 2017, **9**, 14347–14356.
91 Y. N. Wang, Y. H. Lu, J. Y. Zhang, X. F. Hu, Z. Y. Yang, Y. Guo and Y. B. Wang, *J. Mater. Chem. B*, 2019, **7**, 538–547.
92 B. B. Chu, F. Peng, H. Y. Wang, Y. Y. Su and Y. He, *J. Mater. Chem. B*, 2018, **6**, 7378–7382.
93 R. K. Kankala, P. Y. Tsai, Y. Kuthati, P. R. Wei, C. L. Liu and C. H. Lee, *J. Mater. Chem. B*, 2017, **5**, 1507–1517.
94 L. Li, W. Y. Gu, J. Z. Chen, W. Y. Chen and Z. P. Xu, *Biomaterials*, 2014, **35**, 3331–3339.
95 R. Ma, Y. P. Wang, L. Yan, L. L. Ma, Z. G. Wang, H. C. Chan, S. K. Chiu, X. F. Chen and G. Y. Zhu, *Chem. Commun.*, 2015, **51**, 7859–7862.
96 Z. G. Wang, R. Ma, L. Yan, X. F. Chen and G. Y. Zhu, *Chem. Commun.*, 2015, **51**, 11587–11590.
97 N. Wang, Z. G. Wang, Z. F. Xu, X. F. Chen and G. Y. Zhu, *Angew. Chem., Int. Ed.*, 2018, **57**, 3426–3430.
98 X. Mei, W. Wang, L. Yan, T. T. Hu, R. Z. Liang, D. Yan, M. Wei, D. G. Evans and X. Duan, *Biomaterials*, 2018, **165**, 14–24.
99 T. Y. Hu, J. He, S. M. Zhang, X. Mei, W. K. Zhang, R. Z. Liang, M. Wei, D. G. Evans and X. Duan, *Chem. Commun.*, 2018, **54**, 5760–5763.
100 L. Q. Peng, X. Mei, J. He, J. K. Xu, W. K. Zhang, R. Z. Liang, M. Wei, D. G. Evans and X. Duan, *Adv. Mater.*, 2018, **30**, 1707389.
101 W. S. Xie, Z. H. Guo, Z. B. Cao, Q. Gao, D. Wang, C. Boyer, M. Kavallaris, X. D. Sun, X. M. Wang, L. Y. Zhao and Z. Gu, *ACS Biomater. Sci. Eng.*, 2019, **5**, 2555–2562.
102 B. Li, Z. Gu, N. Kurniawan, W. Y. Chen and Z. P. Xu, *Adv. Mater.*, 2017, **29**, 1700373.
103 L. Yan, X. F. Chen, Z. G. Wane, X. J. Zhang, X. Y. Zhu, M. J. Zhou, W. Chen, L. B. Huang, V. A. L. Roy, P. K. N. Yu, G. Y. Zhu and W. J. Zhang, *ACS Appl. Mater. Interfaces*, 2017, **9**, 32990–33000.
104 R. P. Wang, Z. S. He, P. J. Cai, Y. Zhao, L. Gao, W. Z. Yang, Y. L. Zhao, X. Y. Gao and F. P. Gao, *ACS Appl. Mater. Interfaces*, 2019, **11**, 13964–13972.
105 Z. H. Zhao, H. Kantamneni, S. Q. He, S. Pelka, A. S. Venkataraman, M. Kwon, S. K. Libutti, M. Pierce, P. V. Moghe, V. Ganapathy and M. C. Tan, *ACS Biomater. Sci. Eng.*, 2018, **4**, 2350–2363.
106 N. Yang, Y. P. Ding, Y. L. Zhang, B. Wang, X. Zhao, K. M. Cheng, Y. X. Huang, M. Taleb, J. Zhao, W. F. Dong, L. R. Zhang and G. J. Nie, *ACS Appl. Mater. Interfaces*, 2018, **10**, 22963–22973.
107 X. C. Gao, R. X. Cui, G. F. Ji and Z. L. Liu, *Nanoscale*, 2018, **10**, 6205–6211.
108 Y. S. Yoon, B. I. Lee, K. S. Lee, G. H. Im, S. H. Byeon, J. H. Lee and I. S. Lee, *Adv. Funct. Mater.*, 2009, **19**, 3375–3380.
109 Y. Zhang, H. Li, N. Du, S. Song and W. Hou, *Appl. Clay Sci.*, 2017, **143**, 336.
110 Z. Gu, H. L. Zuo, L. Li, A. H. Wu and Z. P. Xu, *J. Mater. Chem. B*, 2015, **3**, 3331–3339.
111 S. X. Shi, B. C. Fliss, Z. Gu, Y. A. Zhu, H. Hong, H. F. Valdovinos, R. Hernandez, S. Goel, H. M. Luo, F. Chen, T. E. Barnhart, R. J. Nickles, Z. P. Xu and W. B. Cai, *Sci. Rep.*, 2015, **5**, 16930.
112 H. L. Zuo, W. Y. Chen, H. M. Cooper and Z. P. Xu, *ACS Appl. Mater. Interfaces*, 2017, **9**, 20444–20453.
113 A. Y. Park, H. Kwon, A. J. Woo and S. J. Kim, *Adv. Mater.*, 2005, **17**, 106–109.
114 J. M. Oh, S. J. Choi, G. E. Lee, S. H. Han and J. H. Choy, *Adv. Funct. Mater.*, 2009, **19**, 1617–1624.
115 P. R. Wei, S. H. Cheng, W. N. Liao, K. C. Kao, C. F. Weng and C. H. Lee, *J. Mater. Chem.*, 2012, **22**, 5503–5513.
116 Y. M. Kuo, Y. Kuthati, R. K. Kankala, P. R. Wei, C. F. Weng, C. L. Liu, P. J. Sung, C. Y. Mou and C. H. Lee, *J. Mater. Chem. B*, 2015, **3**, 3447–3458.
117 L. Yan, W. Chen, X. Y. Zhu, L. B. Huang, Z. G. Wang, G. Y. Zhu, V. A. L. Roy, K. N. Yu and X. F. Chen, *Chem. Commun.*, 2013, **49**, 10938–10940.
118 L. Yan, Y. Wang, J. H. Li, S. Kalytchuk, A. S. Susha, S. V. Kershaw, F. Yan, A. L. Rogach and X. F. Chen, *J. Mater. Chem. C*, 2014, **2**, 4490–4494.
119 D. H. Park, J. Cho, O. J. Kwon, C. O. Yun and J. H. Choy, *Angew. Chem., Int. Ed.*, 2016, **55**, 4582–4586.
120 L. Yan, Z. G. Wang, X. F. Chen, X. J. Gou, Z. Y. Zhang, X. Y. Zhu, M. H. Lan, W. Chen, G. Y. Zhu and W. J. Zhang, *Chem. Commun.*, 2017, **53**, 2339–2342.
121 L. Yan, M. J. Zhou, X. J. Zhang, L. B. Huang, W. Chen, V. A. L. Roy, W. J. Zhang and X. F. Chen, *ACS Appl. Mater. Interfaces*, 2017, **9**, 34185–34193.
122 Z. Gu, J. J. Atherton and Z. P. Xu, *Chem. Commun.*, 2015, **51**, 3024–3036.
123 Q. Yue, Y. Zhang, Y. J. Jiang, J. L. Li, H. W. Zhang, C. Z. Yu, A. A. Elzatahry, A. Alghamdi, Y. H. Deng and D. Y. Zhao, *J. Am. Chem. Soc.*, 2017, **139**, 4954–4961.
124 Y. T. Niu, M. H. Yu, J. Zhang, Y. N. Yang, C. Xu, M. Yeh, E. Taran, J. J. C. Hou, P. P. Gray and C. Z. Yu, *J. Mater. Chem. B*, 2015, **3**, 8477–8485.

Open Access Article. Published on 29 August 2019. Downloaded on 2/10/2026 5:01:13 AM.
This article is licensed under a Creative Commons Attribution 3.0 Unported Licence.

125 J. Liu, S. Z. Qiao, S. B. Hartono and G. Q. Lu, *Angew. Chem., Int. Ed.*, 2010, **49**, 4981–4985.
126 Q. S. Han, X. H. Wang, X. L. Liu, W. Xiao, S. F. Cai, C. Wang and R. Yang, *J. Mater. Chem. B*, 2019, **7**, 1124–1132.
127 X. Y. Cui, W. L. Cheng and X. J. Han, *J. Mater. Chem. B*, 2018, **6**, 8078–8084.
128 J. Wen, K. Yang, X. C. Ding, H. J. Li, Y. Q. Xu, F. Y. Liu and S. G. Sun, *Inorg. Chem.*, 2019, **58**, 2987–2996.
129 H. F. Bao, J. P. Yang, Y. Huang, Z. P. Xu, N. Hao, Z. X. Wu, G. Q. Lu and D. Y. Zhao, *Nanoscale*, 2011, **3**, 4069–4073.
130 J. Liu, R. Harrison, J. Z. Zhou, T. T. Liu, C. Z. Yu, G. Q. Lu, S. Z. Qiao and Z. P. Xu, *J. Mater. Chem.*, 2011, **21**, 10641–10644.
131 J. Wang, J. D. Zhou, Z. S. Li, Y. C. Song, Q. Liu, Z. H. Jiang and M. L. Zhang, *Chem. – Eur. J.*, 2010, **16**, 14404–14411.
132 H. Zhang, D. K. Pan and X. Duan, *J. Phys. Chem. C*, 2009, **113**, 12140–12148.
133 H. Zhang, D. K. Pan, K. Zou, J. He and X. Duan, *J. Mater. Chem.*, 2009, **19**, 3069–3077.
134 D. K. Pan, H. Zhang, T. Fan, J. G. Chen and X. Duan, *Chem. Commun.*, 2011, **47**, 908–910.
135 D. A. Li, Y. T. Zhang, M. Yu, J. Guo, D. Chaudhary and C. C. Wang, *Biomaterials*, 2013, **34**, 7913–7922.
136 M. F. Shao, F. Y. Ning, J. W. Zhao, M. Wei, D. G. Evans and X. Duan, *J. Am. Chem. Soc.*, 2012, **134**, 1071–1077.
137 J. Wang, R. R. Zhu, B. Gao, B. Wu, K. Li, X. Y. Sun, H. Liu and S. L. Wang, *Biomaterials*, 2014, **35**, 466–478.
138 K. Zhao, G. Y. Rong, C. Guo, X. M. Luo, H. Kang, Y. W. Sun, C. X. Dai, X. H. Wang, X. Wang, Z. Jin, S. J. Cui and Q. S. Sun, *Int. J. Nanomed.*, 2015, **10**, 2895–2911.
139 Q. S. Zheng, Y. L. Hao, P. R. Ye, L. Q. Guo, H. Y. Wu, Q. Q. Guo, J. Z. Jiang, F. F. Fu and G. N. Chen, *J. Mater. Chem. B*, 2013, **1**, 1644–1648.
140 C. P. Chen, L. K. Yee, H. Gong, Y. Zhang and R. Xu, *Nanoscale*, 2013, **5**, 4314–4320.
141 X. L. Huo, C. F. Dai, S. P. Li and X. D. Li, *RSC Adv.*, 2015, **5**, 8689–8692.
142 I. Gualandi, Y. Vlamidis, L. Mazzei, E. Musella, M. Giorgetti, M. Christian, V. Morandi, E. Scavetta and D. Tonelli, *ACS Appl. Nano Mater.*, 2019, **2**, 143–155.
143 Y. Wei, S. L. Chen, F. C. Li, Y. Lin, Y. Zhang and L. Liu, *ACS Appl. Mater. Interfaces*, 2015, **7**, 14182–14191.
144 H. Q. Huang, R. Chen, J. L. Ma, L. Yan, Y. Q. Zhao, Y. Wang, W. J. Zhang, J. Fan and X. F. Chen, *Chem. Commun.*, 2014, **50**, 15415–15418.
145 Y. F. Zhao, X. Zhang, X. D. Jia, G. I. N. Waterhouse, R. Shi, X. R. Zhang, F. Zhan, Y. Tao, L. Z. Wu, C. H. Tung, D. O'Hare and T. R. Zhang, *Adv. Energy Mater.*, 2018, **8**, 1703585.
146 M. M. Zhao, Q. X. Zhao, B. Li, H. G. Xue, H. Pang and C. Y. Chen, *Nanoscale*, 2017, **9**, 15206–15225.
147 X. R. Gao, L. X. Lei, L. W. Kang, Y. Q. Wang, Y. W. Lian and K. L. Jiang, *J. Alloys Compd.*, 2014, **585**, 703–707.
148 M. X. Li, Y. Sultanbawa, Z. P. Xu, W. Y. Gu, W. Y. Chen, J. Y. Liu and G. R. Qian, *Colloids Surf., B*, 2019, **174**, 435–442.
149 C. P. Chen, P. Gunawan, X. W. Lou and R. Xu, *Adv. Funct. Mater.*, 2012, **22**, 780–787.
150 D. Hesse, M. Badar, A. Bleich, A. Smoczek, S. Glage, M. Kieke, P. Behrens, P. P. Muller, K. H. Esser, M. Stieve and N. K. Prenzler, *J. Mater. Sci.: Mater. Med.*, 2013, **24**, 129–136.
151 M. Badar, M. I. Rahim, M. Kieke, T. Ebel, M. Rohde, H. Hauser, P. Behrens and P. P. Mueller, *J. Biomed. Mater. Res., Part A*, 2015, **103**, 2141–2149.
152 F. Duda, M. Kieke, F. Waltz, M. E. Schweinefuss, M. Badar, P. P. Muller, K. H. Esser, T. Lenarz, P. Behrens and N. K. Prenzler, *J. Mater. Sci.: Mater. Med.*, 2015, **26**, 5334.
153 F. Peng, H. Li, D. H. Wang, P. Tian, Y. X. Tian, G. Y. Yuan, D. M. Xu and X. Y. Liu, *ACS Appl. Mater. Interfaces*, 2016, **8**, 35033–35044.
154 Y. Q. Shu, P. G. Yin, B. L. Liang, H. Wang and L. Guo, *ACS Appl. Mater. Interfaces*, 2014, **6**, 15154–15161.
155 L. Mao, J. Y. Liu, S. J. Zheng, H. Q. Wu, Y. J. Liu, Z. H. Li and Y. K. Bai, *RSC Adv.*, 2019, **9**, 5834–5843.
156 N. B. Allou, P. Saikia, E. F. Assanvo and R. L. Goswamee, *Polym. Compos.*, 2018, **39**, E1606–E1617.
157 G. Y. Zhu, Y. Long, H. Z. Ren, Y. S. Zhou, L. J. Zhang, Z. H. Shi, F. K. Shehzad and H. M. Asif, *J. Phys. Chem. C*, 2016, **120**, 22549–22557.
158 S. S. Lee, G. E. Choi, H. J. Lee, Y. Kim, J. H. Choy and B. Jeong, *ACS Appl. Mater. Interfaces*, 2017, **9**, 42668–42675.
159 Y. H. Ao, D. D. Wang, P. F. Wang, C. Wang, J. Hou and J. Qian, *RSC Adv.*, 2015, **5**, 54613–54621.
160 V. Rives, E. M. Labajos and M. Herrero, *Polyethylene-Based Blends, Composites and Nanocomposities*, 2015, 163–199, DOI: 10.1002/9781118831328.
161 N. B. Allou, A. Yadav, M. Pal and R. L. Goswamee, *Carbohydr. Polym.*, 2018, **186**, 282–289.
162 Y. P. Zhang, J. W. Ji, H. P. Li, N. Du, S. E. Song and W. G. Hou, *Soft Matter*, 2018, **14**, 1789–1798.
163 L. Yan, A. P. Raphael, X. Y. Zhu, B. L. Wang, W. Chen, T. Tang, Y. Deng, H. J. Sant, G. Y. Zhu, K. W. Choy, B. K. Gale, T. W. Prow and X. F. Chen, *Adv. Healthcare Mater.*, 2014, **3**, 555–564.
164 S. P. Sullivan, D. G. Koutsonanos, M. D. Martin, J. W. Lee, V. Zarnitsyn, S. O. Choi, N. Murthy, R. W. Compans, I. Skountzou and M. R. Prausnitz, *Nat. Med.*, 2010, **16**, 915–920.
165 S. P. Sullivan, N. Murthy and M. R. Prausnitz, *Adv. Mater.*, 2008, **20**, 933–938.
166 Y. X. Chen, R. Zhu, Q. F. Ke, Y. S. Gao, C. Q. Zhang and Y. P. Guo, *Nanoscale*, 2017, **9**, 6765–6776.
167 M. H. Kim, W. Hur, G. Choi, H. S. Min, T. H. Choi, Y. B. Choy and J. H. Choy, *Adv. Healthcare Mater.*, 2016, **5**, 2765–2775.
168 N. Feliu, D. Docter, M. Heine, P. Del Pino, S. Ashraf, J. Kolosnjaj-Tabi, P. Macchiarini, P. Nielsen, D. Alloyeau, F. Gazeau, R. H. Stauber and W. J. Parak, *Chem. Soc. Rev.*, 2016, **45**, 2440–2457.
169 Z. Y. Cai, X. M. Bu, P. Wang, J. C. Ho, J. H. Yang and X. Y. Wang, *J. Mater. Chem. A*, 2019, **7**, 5069–5089.

 This journal is © The Royal Society of Chemistry 2019

170 J. F. Yu, Q. Wang, D. O'Hare and L. Y. Sun, *Chem. Soc. Rev.*, 2017, **46**, 5950–5974.
171 M. Pavlovic, P. Rouster, T. Oncsik and I. Szilagyi, *ChemPlusChem*, 2017, **82**, 121–131.
172 B. R. Smith and S. S. Gambhir, *Chem. Rev.*, 2017, **117**, 901–986.
173 J. Z. Du, H. J. Li and J. Wang, *Acc. Chem. Res.*, 2018, **51**, 2848–2856.
174 M. Zheng, W. Tao, Y. Zou, O. C. Farokhzad and B. Shi, *Trends Biotechnol.*, 2018, **36**, 562–575.
175 M. X. Yu, J. Xu and J. Zheng, *Angew. Chem., Int. Ed.*, 2019, **58**, 4112–4128.
176 J. Q. Wang and G. Liu, *Angew. Chem., Int. Ed.*, 2018, **57**, 3008–3010.
177 D. Tichit, G. Layrac and C. Gerardin, *Chem. Eng. J.*, 2019, **369**, 302–332.

Open Access Article. Published on 29 August 2019. Downloaded on 2/10/2026 5:01:13 AM.
This article is licensed under a Creative Commons Attribution 3.0 Unported Licence.